Interactive comment on "Online gas and particle phase measurements of organosulfates, organosulfonates and nitrooxyorganosulfates in Beijing utilizing a FIGAERO ToF-CIMS" by Michael Le Breton et al.

We thank all the reviewers for their valuable input and critical questions they have posed in which we feel we have answered fully and improved the manuscript in all areas questioned by the reviewers.

Summary of amendments

The main comments from both reviewers for this manuscript regarded the peak fitting and validating the Sulfur Containing Organic (SCO) measurement with the Iodide FIGAERO CIMS. We have addressed this by adding a section in the methodology that details the peak fitting, calibration and validation of the measurement via comparison with offline methods. We have described in further detail how the process of peak fitting with Tofware and how mass calibrants are utilised for accurate peak fitting across the full mass range, which is now illustrated in a supplementary figure displaying each mass calibrant ions error time series varying no greater than +/- 1 ppm for the whole campaign. Discussion of peak fitting the SCOs now details the "custom" peak shape which is utilised that does not assume a Gaussian peak shape in the spectra, further improving the ability to identify individual peaks under multi peak spectral fits and more accurately constrain the centroid value. The peak fitting is further discussed and peak fittings for all SCOs can be found in the supplementary data. The peak fittings here are average peak shapes from the entire field campaigns desorption data. Peak fitting can be performed in a number of different manners and in reality should be performed on many varying "periods" of data which fully represent the campaigns data. Here, we did not want to "cherry pick" the periods of higher SCO concentration to provide better peak fitting results, but rather highlight their significance in the spectra throughout the campaign, but also acknowledge the complexity of peak fitting and the consequential variation in possible error (or LOD issues) when fitting multi peaks. The validation of these peak fits were previously absent from the manuscript due to the comparison to offline methods being shown in an accompanying paper, although we have now included this analysis within the manuscript to illustrate how the peak fits presented can be utilised for accurate SCO measurements. A paragraph and plot have now been added to the manuscript detailing a time series comparison to offline HPLC and orbitrap measurements. The provided results show a good agreement between singular SCOs chosen, IEPOX sulfate and glycolic acid sulfate, with R values of 0.78 and 0.82 respectively. Comparison of the sum of SCOs measured by both orbitrap and HPLC also show good agreement (R = 0.7 and 0.81 respectively) further illustrating that the CIMS is agreeing with offline measurements of SCOs when the data is averaged to diurnal values. The method itself will contain a degree of error due to different locations on site (laboratory and inlet) and missing CIMS data in the analysis daily due to background measurements. The 2 calibrations are fully discussed that firstly prove the ionisation technique is linearly sensitive to SCOs, but also highlight that this instrument can quantify its measurements. Similarly for offline SCO measurement techniques, quantification is a limiting factor due to availability of standards, which also limits the ability for error quantification on the measurement. Here we utilise the two lab calibrants for quantification and error calculation, although we still do note that further work is necessary to improve future work on measurement of SCOs. It is worth noting that current CIMS literature utilises this approach due its ability to measure a vast range of species which do not have standards i.e. Lee *et al.,* (2016) who identify 87 organonitrates. We therefore feel this analysis now confirms to the reader that CIMS can measure SCOs and the subsequent analysis within the manuscript can be approached with confidence.

Fragmentation of SCOs is discussed in more detail citing the literature presenting possible fragmentation issues and subsequent complexities in VP calculations. We conclude that we see fragmentation but stress we report fragmentation of SCOs into smaller ions and not oligomers fragmenting to SCOs of the same mass, which would be observed by a double Tmax desorption peak. We show a figure in the supplementary that illustrates the variation of Tmax for NP OS throughout the campaign and the average thermogram which exhibits no double desorption. We also state that fragmentation to the NP OS mass would require greater energy, which would increase the Tmax temperature and subsequent VP value. We acknowledge that this is the first field data of SCOs and interpretation of Tmax may be more problematic due to uncontrollable variations in field data. Therefore, we limit the analysis of Tmax and VPs to the calibrated NP OS, which we have performed under controlled conditions. The KEMS data supports the possibility for a gas phase presence of SCOs, which we indicate can be extracted from Tmax relative to that for NP OS, although we cannot explain the IEPOX sulfate high VP and therefore believe further analysis into this subject is wanted.

Detailed responses to each reviewer's comment are detailed below with corresponding actions taken within the manuscript.

Anonymous Referee #3

This paper presents the characterization of organic aerosol sampled in Beijing using a FIGAERO ToF-CIMS with a focus on the organosulfates (CHOS and CHONS). In this manuscript, the authors have attempted to quantify these species and look at their distribution between gas and particle phases. While the method/idea proposed in this work is interesting and could lead to a new way to characterize such compounds, this paper cannot be accepted as it is. Indeed, the identification of the OSs is based on peak fittings that are highly questionable. In addition, the authors concluded on the validity of the method/results without any strong support/ evidence. As it is the paper is speculative and major improvements are needed to support this work. The authors seem to have intentionally left crucial information out of this manuscript to write (an)other paper(s). If this current manuscript cannot stand by itself (and it is the case) additional information have to be added.

The first line of the abstract: "Fast" Inlet? The correct name of the FIGAERO is Filter inlet. SCO identification/quantification:

Response: This is correct, it should read filter inlet

Action: This has been amended in the text

There is clearly a lack of information in these sections and more efforts are needed to better describe validate the method/identification

- The mass calibration is crucial in the identification of the compounds, have the authors checked if the parameters didn't change over time? The authors should propose the time series of the parameters in the SI. - The authors need to provide the peak fittings for all of the peaks and not only two compounds. The peaks reported in Figure 1 are very small and poorly resolved, which make the "identification" questionable. If they claim they identified 17 SCOs, they should report 17 HR fittings. In addition, please add the masses and the formula of the compounds observed on the HR fittings. - It is hard to believe that the mass resolution of the instrument was 4000 based on the peak shape/HR fittings proposed in Figure 1. The authors should bring more evidence and make sure the resolution was the same throughout the campaign. - The authors mentioned that they have compared LC-MS and FIGAERO data. Where are these data? They need to be reported in this work. The authors said: “This analysis is not within the scope of this work and provides the basis of the correct identification to which a future paper will probe the caveats observed between the measurement techniques.” It is actually the scope of the paper, demonstrating that the FIGAERO is able to quantify OSs. Therefore comparison with well-known techniques is more than crucial. LC-MS vs FIGAERO should be added ([C],. . .).

Response: The above points are extremely important and have been accounted for in full within the manuscript to ensure the reader that SCOs are indeed being measured. We have now added a new section into the manuscript which aims to validate the measurements to the reader with the methods described by the reviewer. A time series mass calibration plot has been added to the supplementary and described in the text to show that the mass accuracy does not deviate greater or less than 1 and -1 throughout the campaign for the entire mass range. This provides the reader with confidence that correctly identified peaks should have little error related to mass accuracy and indeed peak identification is constantly as accurate as possible throughout the mass range. To aid this, the mass resolution of 3500 is quoted, which was indeed lower than optimum for the ToF CIMS, although was deemed necessary to increase the sensitivity as the X ray source provides a magnitude less ionisation ions than the usual Polonium 235 source.

Peak fittings of all OSs presented in the work have now been added to the supplementary text. The previous fits for figure 1 displayed the average peak fit for all the data over the whole campaign. To better represent the data we have now chosen the average peak fit for only the particle phase data. As we expect little OS in the gas phase, we would have a larger amount of gas phase peaks which would skew the significance of the SCOs. The SCO peaks now represent a significant peak on the spectrum highlighting the accurate peak fitting and representation in the particle phase on the spectra. We also note in the text that peak fitting is performed utilising a standard peak shape representing the data and not assuming a Gaussian peak. This better constrains the residual and the centroid of the peaks. We then calibrate for 2 SCOs to not only confirm the ability to ionise and detect SCOs but also show the ability of CIMS to quantify the measurement.

We have now also included the required comparison between the online and offline measurements of SCOs. A description of how the comparison is performed and example results for several OSs is displayed in supplementary plots. The SCOs measured by the CIMS and orbitrap correlated at the 0.05 significance level, which is stated in the text and again proves that both offline and online measurements significantly correlate. Correlations of example SCOs such as glycolic acid sulfate and IEPOX sulfate between HPLC and CIMS have an R of 0.78 and 0.82. The correlation between 5 overlapping SCOs results in an R value of 0.7.

We believe that by now presenting accurate peak fittings which do not deviate over time and a significant comparison with offline measurements of SCOS that the reader should be fully convinced that the ToF CIMS is indeed measuring SCOs and can therefore have confidence in the subsequent analysis and the ambient observations that is the focus of this manuscript.

Action: A new section has been added to manuscript providing ample evidence of accurate peak identification and quantification of SCOs. Firstly a mass calibrant time series has been provided in

the supplementary showing the error varies less than +/-1 ppm throughout the campaign across the mass range. The mass resolution of 3500 is stated. All peak fittings are provided in the supplementary showing dominant SCO peaks in the spectrum. A comparison of the CIMS measurements to offline SCO measurements has been provided and detailed to show good agreement between the methods at a statistically significant level. The calibration of the 2 SCOs has been then placed into this section to provide further evidence for the reader that all caveats for identification and quantification have been accounted for.

Page 8. Lines 9-12: The authors have to provide this information, that's an important parameter. In addition, we do not know if the ramp chooses during the field campaign leads to high fragmentation or not.

Response: The ramp rate was maintained in the field at the same rate as the calibration of the OS to ensure the same level of fragmentation. The varying degree of fragmentation was discovered post campaign during calibrations, therefore the choice of calibration applied was set to the same ramp rate as for the field measurements. The important message for the reader here is that changing ramp rate will change sensitivity due to fragmentation, which is important to account for during calibration.

Action: This has been clarified as explained in the response.

Page 8. Lines 13-15. The authors mentioned that the OS concentrations are low but in another section that they contribute to a significant fraction page 7 line 14. Make sure your statements are consistent.

Response: The contribution of OS to PM is relatively low but the representation of the OS measured here to total OS assumed from previous work is significant.

Action: This has been reworded to clarify its meaning.

Lines 14-19: The authors discussed the fragmentation issue. It is recognized that the FIGAERO or in general thermo desorption leads to the fragmentation of organic species (Thornton's group, Stark et al., 2017;. . .). While they acknowledged this problem, the authors didn't discuss this point when they determined/discussed the volatility of the OSs (Section 3.2). In the existing literature, previous FIGAERO studies have discussed this potential artifact and mention that the decomposition of oligomers could lead to lower Tmax than expected. Would it be the case for the OSs? The authors compare the volatility of acid compounds between the Knudsen and the FIGAERO. It is interesting but not relevant to the current study as they didn't quantify/look at the carboxylic acids. Have they done the comparison with the OSs used in this study (e.g.LAS & NP OS)? - The authors should provide the Tmax & thermograms for all the SCO and look at the evolution of individual Tmax throughout the campaign.

Response: The discussion of Tmax evolves from the observation of gas phase SCOs. The section discussing Tmax and VPs of the OSs has been reduced to solely discuss the OS calibrated by an independent instrument to confirm the possibility of gas phase OSs by having a semi volatile VP.

The comparison to carboxylic acids serves solely to illustrate that compounds measured ambiently of known VP agree with the KEMS method and therefore provides reliability in scaling of the Tmax values to interpreted VPs. We now do not further probe VPs via Tmax analysis and state that this should firstly be performed in a laboratory, as was performed with NP OS as field data can provide further unresolvable complexities. Nevertheless the data still shows SCOs potential to be in the gas phase, supported by external VP measurements. If fragmentation was to occur by oligomers or dimers, the energy to break these bonds, then to vaporise the fragments would be greater than the energy needed to merely vaporise the OS mass detected and therefore would result in a second Tmax at higher temperatures than the one for OS we observe.

A figure illustrating the thermogram of NP OS and its Tmax values evolution throughout the campaign is now included as requested by the reviewer illustrating little variation in Tmax and no double desorption at this mass occurring from fragmentation.

Action: Further text has been provided to discuss fragmentation and the potential for it to affect determination of the VPs of SCOs, although we conclude that it would result in a higher Tmax for the SCOs, thus underestimating any estimation of VP. We also state no double desorption's are observed for the SCOs and a figure has been included to display stable Tmax values throughout the campaign.

Discussion of Tmax and VP is now limited to calibrated SOCs. The discussion on the comparison of carboxylic acid Tmaxs and VPs has been made more clear to represent them as a benchmark to validate the Tmaxs in this work illustrating the agreement with VPs from the KEMS, thus providing confidence in the KEMS SCO VP measurement.

Page 9. The authors should provide simple analysis before going into too many details to validate the FIGAERO data (e.g. sum of organics vs OA; sum of organics vs SO4; sum of SCO vs OA, SO4,. . .).

Response: The papers aim is to focus on organic sulphates sources and production in the ambient atmosphere. This is a novel approach and new analysis utilising this instrument. The CIMS is also specialised on single compound identification and not the sum of organics, so it likely to greatly underestimate the organic mass compared to OA. Therefore, we do not feel this analysis will provide further useful insights in the analysis of this work.

Action: No pre analysis has been placed into the paper due to the focus on SCOs. We have indicated in the paper that this analysis can be performed, although we are aware that the selectivity of the ionisation scheme inhibits CIMS to see all of the organic mass.

Page 10. Lines 30-34. How is it possible that IEPOX-OS could be more volatile than less oxidized compounds, such as GAS? If it was the case previous measurements realized by Stone's group in the SE-US would have revealed such phenomena. Overall this discussion is lacking comparisons with previous studies (Lopez-Hilfiker et al., 2016; Hettiyadura et al., 2017) and evidence/better constraints to validate such "results".

Response: This is a very valid point to which we must address. Due to the limitation of laboratory calibrated SCOs (limited by standard availability), we have now limited the discussion of the VPs of SCOs. The calibration of NP OS via the KEMS instrument and FIGAERO indicate a semi volatile vapour pressure for the SCO. It is through extrapolation of this knowledge that other SCOs would have a relatively varying VP via comparison of their Tmax. Although we acknowledge that these other SCOs have not been calibrated, therefore we have removed the discussion of other SCOs VPs and table 3. We however believe the calibration using the KEMS instrument indicating the potential for gas phase SCOs is an important result from this work and can further lead to a new field of research both for VP calculations of SCOs utilising the FIGAERO and mechanistic understanding of SCO processes.

Action: The manuscript text is now limited to discussion of the VPs of SCOs which have been calibrated in the laboratory, NP OS. We then state that with proper calibration of SCOs, the Tmax and VPs can lead to further discussion of the utilisation of the FIGAERO for partitioning analysis of SCOs.

Page 11. Lines 23-26: That is not true. Liu et al. 2017, ACP reported the formation of such OS from the photooxidation of cyclohexene.

Response: This is correct and must be amended in the text

Action: The text has been amended to account for this

Anonymous Referee #1

This paper describes the application of a FIGAERO ToF-CIMS to the characterisation of organic aerosol in Beijing, with a specific emphasis on the heteroatom containing CHOS and CHONS groups. The authors have attempted to quantify these species during a field campaign and then compare the temporal evolution to various chemical and metrological factors. I have no issue with the methods used to try and understand the data in the later part of the paper. While the idea has merit, and would be a very useful addition to the field, I cannot accept that the technique is actually measuring the species of interest based on the data provided in this paper. The extraction of very small and obscured signals from poorly resolved peaks, exemplified for the two OS species in Figure 1, has not been justified in any way. The description of the peak deconvolution is short and contains no evidence that this method has been validated. Have the authors measured the mass resolution to ensure that it really is 4000? The peaks widths used in the fitting require this to be known and the mass calibration across the entire range has to have sufficient accuracy. Has this approach been tested in the lab or are there previous publications? Also no uncertainties are provided. The entire paper and conclusions rests entirely on this component and as such I cannot recommend this paper be accepted to ACP at present. There is mention of a comparison to offline methods in the paper as being "outside the scope of this work". To me this is absolutely critical to provide validation of the method.

Response: We have now added a new section into the manuscript which aims to validate the measurements to the reader with the methods described by the reviewer. A time series mass calibration plot has been added to the supplementary and described in the text to show that the

mass accuracy does not deviate greater or less than 1 and -1 throughout the campaign for the entire mass range. This provides the reader with confidence that correctly identified peaks should have little error related to mass accuracy and indeed peak identification is constantly as accurate as possible throughout the mass range. To aid this, the mass resolution of 3500 is quoted, which was indeed lower than optimum for the ToF CIMS, although was deemed necessary to increase the sensitivity as the X ray source provides a magnitude less ionisation ions than the usual Polonium 235 source.

Peak fittings of all OSs presented in the work have now been added to the supplementary text. The previous fits for figure 1 displayed the average peak fit for all the data over the whole campaign. To better represent the data we have now chosen the average peak fit for only the particle phase data. As we expect little OS in the gas phase, we would have a larger amount of gas phase peaks which would skew the significance of the SCOs. The SCO peaks now represent a significant peak on the spectrum highlighting the accurate peak fitting and representation in the particle phase on the spectra.

We have now also included a necessary comparison between the online and offline measurements of SCOs. A description of how the comparison is performed and example results for several OSs is displayed in supplementary plots. The SCOs measured by the CIMS and orbitrap correlated at the 0.05 significance level, which is stated in the text and again proves that both offline and online measurements significantly correlate.

Calibration of the 2 SCOs then follows the comparison to further illustrate the ability of the CIMS to accurately measure and quantify the SCOs. The laboratory calibration of NP OS in the paper highlight the ability for CIMS to measure OSs and with a high sensitivity, which would have also previously been assumed as the iodide ionisation scheme has a high affinity to sulphuric acid.

The uncertainty for the calibrated NP OS is stated to apply for all OS. We acknowledge in the paper that without direct calibration it is difficult to provide an accurate error for all species. This is similar to that applied for 87 organonitrates by Lee et al. (2016) therefore we feel that this method is quite standard for this instrument within the literature.

We believe that by now presenting accurate peak fittings which do not deviate over time and a significant comparison with offfline measurements of SCOS that the reader should be fully convinced that the ToF CIMS is indeed measuring SCOs and can therefore have confidence in the subsequent analysis.

Action: This is the same addition to the responses to reviewer 1:

A new section has been added to manuscript providing ample evidence of accurate peak identification and quantification of SCOs. Firstly a mass calibrant time series has bene provided in the supplementary showing the error varies less than +/-1 ppm throughout the campaign across the mass range. The mass resolution of 3500 is stated. All peak fittings are provided in the supplementary showing dominant SCO peaks in the spectrum. A comparison of the CIMS measurements to offline SCO measurements has bene provided and detailed to show good agreement between the methods at a statistically significant level. The calibration of the 2 SCOs has been then placed into this section to provide further evidence for the reader that all caveats for identification and quantification have been accounted for.

General comment:

Within the text both OS and SCO are used. Are these meant to be different things? It is hard to work out if they are being used interchangeably. The results section contains a large number of typos and some very unclear sentences.

Response: This has been acknowledged and will be amended in the text

Action: The use of SCO and OS has been adjusted in the text to better represent its use i.e. to define possible structural differences in the correct context

Specific comments

Abstract, line 33: "biogenic emissions contributed to only 19 % of the total SCO detected." While understand you want to make a split between these two sources, this is very much dependent of the spread of SCO you measure. Previous offline MS studies of OS in China, such as Wang et al., 2016 identified over 200 OS species in PM2.5. Therefore, your limited subset is very much biased depending on the choice of OS included, in this case only 17 species. You need to be very careful about making generalisation about the relative strength of the two sources based on this. Also, the C10H16NSO7 ion usually appears as a series of peaks in offline HPLC analysis and therefore is better described as monoterpene derived.

Response: This is a very important factor which we must address better. The offline measurements of OSs by orbitrap and HPLC come to a similar conclusion, which includes a large suite of OSs detected. The parallel offline analysis utilises 34 OSs for their analysis and found that anthropogenic OSs were 4 times more abundant than the biogenic OSs.

Action: The text now acknowledges this potential issue but provides information that the offline methods also come to this conclusion upon analysis of the 34 OSs utilised in analysis.

Page 6: SCO identification: There's not enough information here as outlined above. If this instrument has a mass resolution of 4000 (which is not explicitly stated) then at m/z 287, the minimum peak separation ΔM, which allows two ion species to be distinguished, should be around 0.07. Thus in figure 1 (top, right), the light blue and yellow ions should be better resolved. How are the peak centroids determined? The precision in which the intensity of very low s/n OS peaks (where the measured ion signal shows no evidence of this ion) can be retrieved is likely to be very poor. See Cubison and Jimenez, 2015.

Response: The average mass resolution for a standard peak throughout the campaign was 3500, which was lower than optimum (4000) due to a sacrifice of resolution to increases sensitivity for tuning with the new X ray ionisation source, which provides a magnitude less ionisations ions than Polonium210. The peak fittings in the top panel of figure were single point peak fits for the whole dataset. These have now been replaced with more representative standard peak fittings for the data, which are for particle phase measurements only (not including gas phase peak fittings as before which would always include much lower OS counts).

Action: The mass resolution of 3500 is stated in the text and description of the peak fitting and what spectra are used is more accurately described. We state the current issue with CIMS that during analysis peak fittings and accuracy may change due to the changing intensity of co-existing peaks under the same bulk peak. We do however fit a custom peak shape to the spectra to ensure that the residual is not assuming a Gaussian fit, creating a higher accuracy when fitting a centroid to the peak position.

Figure 1: The figure is difficult to understand and read. Why in the middle left hand panel have you not zoomed in so the labelled peaks can be observed? Also, the bottom plot does not really convey any information that is useful to the reader. The I- spectra seems irrelevant to the data being presented. Are there any peaks where the OS dominates the observed ion, rather than being a very small obscured peak? Table 1 and 2: I am confused why there are two tables showing very similar information. Both tables contain a "mean" value but they are different? For example C11H11SO7 has the same mean %OA and %SCO in both tables but different mean concentrations (by a large amount 40 ng m-3 v 120 µg m-3)

Response: We agree with this comment and will amend the tables and figure to represent the data in a more concise, clear and informative manner

Action: Table 1 and 2 have now been merged and the data represented should be more clear and concise. Figure 1 has now been amended to remove the whole I- spectrum. The peaks displayed in the top panels now illustrate peaks from high and low masses on the spectrum. The peak fittings now represented in the supplementary data show SCO ions that have significant peak counts as we now exclude gas phase spectra from this analysis.

Page 7, line 26: There doesn't appear to be any sulphur compounds in your reaction mixture?

Response: The mixture stated as trioxide pyridine was actually sulphur trioxide pyridine.

Action: This information has been added to the text

Page 8, line 4: Figure 2 doesn't actually show a three-point calibration. It shows the peaks obtained for three concentrations but it does show a calibration curve comparing concentration with response.

Response: A 3 point calibration is now shown in the figure

Action: Figure 2 has been amended to now illustrate the thermogram for 3 different mass loadings on the filter and their respective spectra highlighting peaks observed during desorption and also a 4 point calibration curve (1 extra point for background desorption) with NP OS molecules plotted on the x axis and ion counts per desorption on the y axis.

Page 8, line 14-21: I don't follow the reasoning that the low concentration of OS relative to the organic precursors results in little error. I would like to see some examples of the double thermogram and know how widespread this effect is. Can you provide evidence that using only 1 species to determine the error is valid?

Response: This was caused due to typographic error within the text. The text was supposed to state little contribution of organic peak produced relative the OS (i.e. it was reported the wrong way around)

Error calculations are difficult without laboratory standards for calibrations to accurately calculate the error. It is common practise within CIMS literature to utilise a calibration for a functional group (such as organonitrates in Lee et al., 2016) and with that assume the same error. We therefore have applied a large error to account for this possibly varying parameter.

Action: This text has been amended and the application of one error constant has been explained more concisely.

Page 8, line 27: This statement only holds true for species that desorb below 250 C

Response: This point is valid and must be stated within the text.

Action: This has now been acknowledged within the text.

Page 10, line 3: I do not understand this sentence at all. Quite often through the paper sentences are not very direct and contain many extra words.

Response and action: This sentence has been removed due to extensive changed within this section prompted by the reviewer's comments regarding potential inaccuracies of gas phase SCO presence. Overall, the text has been revised to reduce the numbers of words and make the text more concise and effective

Page 10, line 30: What does "mean presence" mean? Again this section lack clarity. I don't think a p:g ratio can be "prominent"? What is the 7.1 % referring to?

Response and action: This line has now been removed due to the removal of VP analysis of uncalibrated SCOs

Page 11, section 4.1: I assume the PTR-MS measurements have been converted to daily averages? This is what the figure seems to present. The sentence starting on line 20 is very long and doesn't make sense. You are not measuring an attribution but using the measurements to test your attribution. Why do you give average toluene mixing ratios and then change to benzene? Be very clear here you are talking about your 17 SCO only.

Response: Yes they have been converted to daily averages. The inclusion of toluene was a typographic error.

Action: This sentence has been clarified and now correctly reports PTR-MS measurements of benzene and isoprene. It now reads "Thus, as shown in Figure 5, PTR-MS measurements mean daily concentrations of benzene and isoprene were utilized to evaluate if the ratio benzene and isoprene can be related to the contribution of aromatic and biogenic SCOs measured in this work"

Page 11, section 4.1.1: Green leaf volatiles and sesquiterpenes have also been identified as biogenic OS sources.

Response and action: This work has now been acknowledged and the reference to Shalmzari et al., (2014) has been added to the text.

Page 12, section 4.1.2: I cannot see any of the trends you discuss here in Figure 6. You don't include any diurnal profiles, only a full time series and therefore the temporal evolution is not clear. At the end of the section I was confused as to whether you thought the NP OS concentration was driven by traffic (hence the second peak) or biomass burning? I guess in reality it's a combination of the two, but this needs to be clearer.

Response: The NP OS from biomass burning from more aged air masses has had time to oxidise and produce the NP OS whereas local sources of NP (biomass burning and traffic) indeed can be sources of NP OS but as they are fresher sources, are less oxidised, and therefore produce much lower signals of NP OS compared to the aged BB air masses.

Action: NP AND NP OS diurnal profiles have now been added to the supplementary data to support the analysis within this section. The text has been made clearer to indeed indicate that both traffic and biomass burning can be a source of SCOs, although the local sources are fresher and hence provide lower mixing ratios of the secondary product.

Figure 2: The legend says "time series" but none of the plots have a time axis? Should say these are m/z intensities. Is the average stick spectrum collected at the desorption temperature with the highest ion count?

Response and action: The caption now reads" Figure 2. The desorption profile of NP OS 3 step calibrations for 0.1 µl, 0.2 µl and 0.3 µl 1000 ppm solution is displayed in the bottom panel and its corresponding average stick spectrum (top left) and sum of counts per molecule loading for each calibration (top right)". The spectrum is an average of the whole desorption profile.

Figure 3: The SCO times series coloured by time is really hard to see when sitting on top of the other signals. I would separate these out.

Response and action: Figure 3 has been amended to display the SCOs on a separate plot panel to the AMS organic and sulfate data.

Figure 5: this legend needs work. The benzene to isoprene ratio is on the lower panel not the upper one. The AMS data is in the upper panel and should be stated. How does the anthropogenic SCO concentration change with the b:iso ratio? Most of the variability seems to be driven by the unknowns.

Response and action: Figure 5 has been amended so the legends are now clear and concise. Although not a dominating factor in the plot, the anthropogenic SCOs also follow a similar time series trend as the benzene:isoprene ratio, similar to what can be seen by the unknowns.

Online gas and particle phase measurements of organosulfates, organosulfonates and nitrooxyorganosulfates in Beijing utilizing a FIGAERO ToF-CIMS

Michael Le Breton[1], Yujue Wang[2], Åsa M Hallquist[3], Ravi Kant Pathak[1], Jing Zheng[2], Yudong Yang[2], Dongjie Shang[2], Marianne Glasius[4], Thomas J Bannan[5], Qianyun Liu[6], Chak. K. Chan[7], Carl. J. Percival[8], Wenfei Zhu[9,] Shengrong Lou[9], David Topping[5], Yuchen Wang[6], Jianzhen Yu[6], Keding Lu[2], Song Guo[2], Min Hu[2] and Mattias Hallquist[1]

[1] Department of Chemistry and Molecular Biology, University of Gothenburg, Gothenburg, Sweden
[2] State Key Joint Laboratory of Environmental Simulation and Pollution Control, College of Environmental Sciences and Engineering, Peking University, Beijing, China
[3] IVL Swedish Environmental Research Institute, Gothenburg, Sweden
[4] Department of Chemistry and iNANO, Aarhus University, 8000 Aarhus C, Denmark
[5] Centre for Atmospheric Science, School of Earth, Atmospheric and Environmental Science, University of Manchester, Manchester, UK
[6] Division of Environment and Sustainability, The Hong Kong University of Science and Technology, Clearwater Bay, Kowloon, Hong Kong
[7] (School of Energy and Environment, City University of Hong Kong, Hong Kong
[8] Jet Propulsion laboratory, Pasadena, California, USA.
[9] Shanghai Academy of Environmental Sciences, Shanghai 200233, China

Correspondence to: M. Le Breton (Michael.le.breton@gu.se) and S. Guo (guosong@pku.edu.cn)

Abstract. A Time of Flight Chemical Ionisation Mass spectrometer (CIMS) utilizing the ~~Fast~~Filter Inlet for Gas and AEROsol (FIGAERO) was deployed at a regional site 40 km north west of Beijing and successfully identified and measured 17 sulfur containing organics (SCOs = organo/nitrooxyorgano sulfates and sulfonates) with biogenic and anthropogenic precursors. The SCOs were quantified using laboratory synthesized standards of lactic acid sulfate and nitrophenol organosulfate (NP OS~~).~~): The variation in field observations were confirmed by comparison to offline measurement techniques (orbitrap and HPLC) using daily averages. The mean total (of the 17 identified by CIMS) SCO particle mass concentration was ~~207 ± 106~~210 ± 110 ng m^{-3} and had a maxima of ~~542~~540 ng m^{-3}, although contributed to only 2 ± ~~2.8~~1% of the organic aerosol (OA)~~. SCO contribution to submicron mass (PM$_1$) indicates a dominant secondary production of SCO due to the low contribution of SCOs to PM$_1$ during periods of high mass loading.~~ The CIMS identified a persistent gas phase presence of SCOs in the ambient air, which was further supported by ~~post campaign~~separate vapour pressure measurements of NP OS~~.~~ by a Knudsen Effusions Mass Spectrometer (KEMS). An increase in RH ~~appeared to promote~~promoted partitioning of SCO to the particle phase whereas higher temperatures favored higher gas phase concentrations. ~~On average 12% of the total SCOs were observed in the gas phase with C$_{10}$H$_{16}$NSO$_7$ having just 5% and IEPOX OS having 44% on average in the gas phase.~~

Biogenic emissions contributed to only 19% of total SCOs ~~detected.~~analysed in this study. Here $C_{10}H_{16}NSO_7$, ~~an alpha-pinene~~a monoterpene derived SCO, representing the highest fraction (10%) followed by an isoprene-derived SCO. The Anthropogenic SCOs with PAH and aromatic precursors dominated the SCO mass loading (51~~% total SCOs)~~%) with $C_{11}H_{11}SO_7$, derived from methyl napthalene oxidation, contributing to 40 ng m^{-3} and 0.3% of the OA mass. ~~Biomass burning was also identified as a potential anthropogenic and biogenic source of SCOs, based on nitrophenol (NP) and acetonitrile time series via secondary production of NP OS.~~

~~Gas and particle phase measurements of glycolic acid suggest that partitioning towards the particle phase promotes glycolic acid sulfate production, contrary to the current formation mechanism suggested in the literature. Highly oxidised multifunctional organic compounds (HOMS) and RO_2 radical diurnal profiles, as measured by the iodide ToF-CIMS, are similar to that of total SCOs, supporting results that indicate HOMS are able to play a role in SCO production.~~ Anthropogenic related SCOs correlated well with benzene, although their abundance depended highly on the photochemical age of the air mass, tracked using the ratio between pinonic acid and its oxidation product, acting as a qualitative photochemical clock. In addition to typical anthropogenic and biogenic precursor the biomass burning precursor nitrophenol (NP) provided significant level of NP OS. It must be noted that the contribution analysis here is only representative of the SCOs detected, where there are likely to be many more SCOs present which the CIMS has not identified.

Gas and particle phase measurements of glycolic acid suggest that partitioning towards the particle phase promotes glycolic acid sulfate production, contrary to the current formation mechanism suggested in the literature. ~~The~~Furthermore, the $HSO_4.H_2SO_4^-$ cluster measured by the CIMS was utilized as a qualitative marker for acidity and ~~provides further evidence~~indicates that the production~~ rate~~ of total SCOs is efficient in highly acidic aerosols with high SO_4^{2-} and organic content. This dependency becomes more complex when observing individual SCOs due to variability of specific VOC precursors.

1. Introduction

Atmospheric particulate matter (PM) is ~~well~~ known to play a major role in ~~adversely~~ affecting ~~the~~climate and air quality~~ and climate~~ leading to severe health issues, such as respiratory and cardiovascular degradation (Pope *et al.*, 2002; 2011; Kim *et al.*, 2015). Secondary organic aerosols (SOA), formed through reactions of volatile organic compounds (VOCs) yielding semi volatile products that partition into the aerosol phase, represents a significant fraction of PM (Hallquist *et al*., 2009) and remains the most poorly understood PM source (Foley *et al*., 2010) due to the complexity of its chemical nature, resulting in discrepancies between observations and models (Heald *et al*., 2005). Annual average PM_1 (particulate matter of diameter less than 1 micron) concentrations in Beijing reached 89.5 µg m^{-3} in 2013 and, although recently dropped to 80.6 µg m^3, is still significantly above the Chinese National Ambient air quality Standard (CNAAQS, 35 µg m^3 annual average). The knowledge gap of ~~emissions and~~ PM primary emissions and secondary production limits scientifically based abatement strategies targeting effects of secondary pollution ~~that significantly contributes to PM~~ in highly polluted regions (Hallquist *et al.*, 2016; Zhang *et al.*, 2012a). Therefore, Beijing is an ideal case study region for intense measurement campaigns to increase our understanding of the sources and processes involved in atmospheric aerosol chemistry in megacities~~ and therefore providing the information necessary to implement mitigation strategies for Pan-Euroasian and Chinese societies.~~. A growing number of field studies in this region have been performed in recent years, specifically focused on the haze events investigating the composition of primary and secondary particle aerosols and their formation mechanisms (Guo *et al.*, 2012, 2014, 2013; Huang *et al*., 2010; Hu *et al.*, 2016, 2017; Li *et al.*, 2017).

Organosulfates (OSs~~)~~), here part of sulfur containing organics (SCOs), are known important SOA components formed by reactions between reactive organic compounds and sulfate (Iinuma *et al.*, 2007; Surratt *et al*., 2007, 2008), which is generated by the oxidation of SO_2, primarily emitted by fossil fuel combustion (Wuebbles and Jain, 2001). OSs have previously been measured in ambient aerosols at a number of ~~varying~~ geographical locations, from ~~the~~ remote regions to highly populated urban environments (Surratt *et al*., 2007, 2008; Kristensen *et al.*, 2011; Stone *et al*., 2012; Zhang *et al*., 2012b; Worton *et al*., 2013; Shalamzari *et al*., 2013; Hansen *et al*., 2014) ~~and also estimated using an AMS (Huang *et al*., 2015),~~ although their composition and contribution to organic mass can vary significantly~~.~~ (Huang *et al*., 2015). To date, ~~a large number~~several of ~~OSs have been identified across the world, although not all~~ their precursors are not known (e.g. Hansen *et al*., 2014). Mechanistic studies reveal multiple possible pathways for ~~OS~~SCO formation, which depend on availability of reactants in the atmosphere (Hettiyadura *et al*., 2015), increasing the complexity of understanding their occurrence and ~~abundance~~descriptions within models. Measurements of ~~individual OSs~~specific SCOs have shown they may individually contribute up to 1% of the total organics (Olson *et al*., 2011; Liao *et al.*, 2015~~), indicating that the total OS contribution is comprised of many different species, which in turn will differ geographically due to emission sources and reaction pathways.~~).

Isoprene ~~OSs~~SCOs are hypothesized to be the most abundant precursor in the ambient atmosphere (Surratt *et al.*, 2007; Liao *et al.*, 2015) and are often used as markers of isoprene-derived SOA in field campaigns (Zhang *et al*., 2012b). Aromatic ~~OSs~~SCOs, considered to originate from anthropogenic sources, have been recently observed in Lahore, Pakistan (Stone *et al*., 2012) and in urban sites in East Asia (Lin *et al*., 2012~~) and are considered to originate from anthropogenic sources.~~). Riva *et al*. (2015 and 2016) have also previously probed the ~~OS~~SCO formation potential from PAH and alkane oxidation in the ~~presecence~~presence of acidic sulfate aerosols. Glycolic acid sulfate (GAS) is considered another potentially important ~~OS~~SCO due to its common abundance and possible sources (Olson *et al*., 2011; Liao *et al*., 2015). It is thought to form via a gas phase precursor reaction with an acidic aerosol sulfate ~~and also~~or from the particle phase reaction of methyl vinyl ketone with a sulfate particle, although both of these mechanisms are yet to be proven (Liao *et al*., 2015). GAS is also the only ~~OS~~SCO to date, which has been detected in the gas phase (Ehn *et al*., 2010), providing possible importance of gas to particle phase partitioning of some ~~OSs.~~ SCOs.

~~OSs~~SCOs are thought to be good tracers for heterogeneous aerosol phase chemistry and SOA formation since the known formation mechanisms involve reactive uptake of gas phase organic species onto aerosol (Surratt *et al.*, 2010). Due to their hydrophilic nature, polarity and relatively low volatility, they may significantly help nanoparticle growth and increase their potential to become cloud condensation nuclei (Smith *et al*., 2008). Therefore, it is imperative to improve our knowledge of ~~OS~~SCO abundance, formation, distribution, precursors and fate to help develop our understanding of SOA formation.

Mass spectrometry coupled with electrospray ionization is a common method to detect ~~OSs~~SCOs (Iinuma *et al*., 2007; Reemtsma *et al*., 2006; Surratt *et al*., 2007; Gomez-Gonzalez *et al*., 2008~~) via the identification of the bisulfate ion, a fragment ion of OSs.~~). Liquid chromatography ~~mass spectrometry is known to~~can efficiently separate aromatic and monoterpene derived organic sulfates containing aromatic rings or long alkyl chains and is ~~therefore another suitable technique~~used for ~~OS detection~~speciation of SCOs (Stone *et al*., 2012). ~~Hydrophilic~~Furthermore, hydrophilic interaction liquid chromatography has ~~also~~ been utilized as a very selective technique due to its ability to allow the ~~OS~~SCO to retain a carboxyl group, enabling detection of a larger suite of compounds (Gao *et al.*, 2006). The methods above often rely on sampling filters taken in the field and therefore provide a relatively low measurement frequency. This can limit the ability to evaluate production pathways when concentrations are often integrated over a period of hours or more. Further reactions on filters between the organics and sulfates has also been postulated to add a bias to the ~~OS~~SCO concentration measured with respect to initial deposition onto the filter (Hettiyadura *et al*., 2017; Kristensen *et al*., 2016). Recently, a Particle Analysis Laser Mass Spectrometer (PALMS) was utilized to measure a number of OSs over the United States highlighting the ability of time of flight mass spectrometers to measure several ~~OSs~~SCOs at high time frequencies (Liao *et al*., 2015).

This study utilizes a Filter Inlet for Gas and AEROsol (FIGAERO) Time of Flight Chemical Ionisation Mass Spectrometer (ToF-CIMS) for the measurement of ambient ~~sulfur containing organics (~~SCOs~~)~~ at a semi-rural site 40 km from Beijing, China. This instrument enables ~~sampling~~measurements of either the gas-phase components or thermally desorbed particles by a high resolution mass spectrometer via a multi-port inlet, as described in detail by Lopez-Hilfiker *et al.*, (2014). The soft and selective ionization technique and high time resolution coupled with the FIGAERO enables the simultaneous detection and measurement of SCOs in the gas and particle phase ~~to~~at ng m^{-3} concentrations. This work aims to identify dominant SCOs in Beijing and their precursors. The high time resolution measurements are utilized to ~~further~~ probe their ~~formation and~~ abundance under different chemical and environmental regimes providing insight into their formation.

2. Experimental

2.1 Site description

The data presented here was collected during the measurement campaign "Photochemical smog in China" with an initiative to enhance our understanding of SOA formation via photochemical smog in China (Hallquist *et al.*, 2016). The campaign was coordinated by Peking University (PKU) and University of Gothenburg with focus on spring/summertime episodic pollution episodes in Northeast China through gas and particle phase measurements. ~~Here we briefly describe the measurement site and instrumental setup for data which is incorporated in this work.~~ The setup was situated at a semi-rural site 40 km North East of downtown Beijing close to Changping town (40.2207° N, 116.2312° E). All on-line instruments sampled from inlets on the 4th floor laboratory (12 metres above ground) at Peking University Changping Campus from the 13th May to 23rd June 2016, while filter measurements took place on the roof. The average temperature and humidity throughout the campaign were 23°C and 44% respectively. The wind speed averaged at 2 ms^{-1} from the South-South West. A total of 4 pollution episodes were observed during the campaign period, which are classified as sustained periods of high aerosol loading reaching a maximum of 115 micrograms per cubic meter (µg m^{-3}). The episodes were dominated by organic and nitrate aerosols although episode 3 contained high sulfate loading, equal to that of nitrate. The mass loading for the semi-rural site showed good correlation with the ~~city~~PKU campus measurement site (30 km South-South-West of the Changping site and 12 km North West of downtown Beijing) throughout the campaign allowing for extrapolation of the semi-rural site results to inner city conditions. HYSPLIT back trajectory results showed the pollution episodes often correlated with air masses coming from the direction of Beijing (South-South-East). Clean air days were mostly North Westerly winds with clean air coming from the rural mountain regions North West of Beijing and the measurement site.

A high resolution ~~(4000)~~ Time of Flight Aerosol Mass Spectrometer (ToF-AMS) was utilized to measure the mass concentrations and size distributions of non-refractory species in submicron aerosols, including organics, sulfate, ammonium and chloride (DeCarlo *et al., 2006*; Hu *et al.*, 2013). The setup of this instrument has been previously described by Hu *et al.* (2016). An Ionicon Analytik high sensitivity PTR-MS (Proton TRansfer Mass Spectrometer) as described by de Gouw and Warneke *et al.*, (2007) provided supporting precursor VOC measurements.

2.3 ToF-CIMS setup

Gas and particle phase ~~ambient~~ species were measured using an iodide ToF-CIMS coupled to the FIGAERO inlet (Lopez-Hilfiker *et al.*, 2014). The ToF-CIMS can be operated in either negative or positive ionization modes, and a variety of reagent ion sources can be used. In this work the ToF-CIMS was operated in single reflection mode. The negative Iodide ion (I^-) was used as the reagent in all experiments. Dry UHP N_2 was passed over a permeation tube containing liquid CH_3I (Alfa Aesar, 99%), and the flow was passing a Tofwerk X-Ray Ion Source type P (operated at 9.5 kV and 150 µA) to produce the ionization ions. The ionized gas was then ~~carried out of the ion source and into~~directed to the IMR through an orifice (Ø = 1 µm). Reaction products (e.g., compound X) were identified by their corresponding cluster ions, XI^- or the deprotonated ion, allowing for the collection of whole-molecule data. The nominal reagent and sample flow rates into the Ion-Molecule Reaction (IMR) chamber of the instrument were 3.5 liters per minute (LPM) and 2 LPM respectively. The IMR itself was temperature controlled at 40˚C and operated at a nominal pressure of 500 mbar. The ToF-CIMS was configured to measure singularly charged ions with a mass to charge ratio (*m/z*) of 7 – 620, a reduced mass range in order to compensate for the lower count rate emitted by the soft X-ray source with respect to the Polonium-235 radioactive source as commonly deployed. The tuning was optimized to increase sensitivity, which resulted in a spectral resolution of 3500. The mass range was at some instances during the campaign changed to a higher mass range (1000 *m/z*) to ensure no major contributing peaks were being unaccounted for. Perfluoropentanoic acid was utilised as a mass calibrant up to *m/z* 527 through its dimer and trimer. This range of mass calibration peaks also limited accurate peak identification above *m/z* 620.

2.4 FIGAERO inlet

The FIGAERO inlet collected particles on a Zefluor® PTFE membrane filter. The aerosol sample line was composed of 12 mm copper tubing, while 12 mm Teflon tubing was used for the gas sample line. The FIGAERO was operated in a cyclic pattern; 25 minute of gas phase sampling and simultaneous particle collection, followed by a 20 minute period during which the filter was shifted into positioned over the IMR inlet and the collected particle mass was desorbed. Desorption was facilitated by a 2 LPM flow of heated UHP N_2 over the filter. The temperature of the N_2 was increased from 20 to 250˚C in 15 minutes (3.5˚C min^{-1}), followed by a 5 minute temperature soak time to ensure that all remaining mass that volatilizes at 250˚C was removed from the filter. The resulting desorption time series profiles allowed for a distinct separation of measured species as a function of their thermal properties. ~~The ToF-CIMS was configured to measure singularly charged ions with a mass to charge ratio (*m/z*) of 7 – 620, a reduced mass range in order to compensate for the lower count rate emitted by the soft X-ray source with respect to the Polonium-235 radioactive source as commonly deployed. The mass range was changed during the campaign to view to a higher mass range (1000 *m/z*) to ensure no major contributing peaks were being unaccounted for. Perfluoropentanoic acid was utilised as a mass calibrant up to *m/z* 527 through its dimer and trimer. This range of mass calibration peaks also limited accurate peak identification above *m/z* 620.~~

Formatted: Indent: Left: 0 cm

2.5 ~~Knudsen Effusion Mass Spectrometer (KEMS)~~

Formatted: English (U.S.)

~~The KEMS technique was utilized to measure the vapour pressure (vapour pressure) of potential gas phase SCOs measured by the CIMS. This technique is able to measure vapour pressures from~~ ~~10^{-1} to 10^{-8}~~ ~~Pascals (Pa) ranging from volatile organic compounds to extremely low volatility organic compounds. A full description of the technique can be found in Booth *et al.* (2009, 2010) and the measurements of a series of compounds over a large VP range, in a recent inter-comparison study from this instrument can be found in Krieger *et al.* (2017). Briefly, the instrument~~

~~consists of a temperature controlled Knudsen effusion cell, suitable for controlled generation of a molecular beam of the sample organic compounds in a vacuum chamber, coupled to a quadrupole mass spectrometer. The cell has a chamfered effusing orifice with a size ≤1/10 the mean free path of the gas molecules in the cell. This ensures the orifice does not significantly disturb the thermodynamic equilibrium of the samples in the cell (Hilpert, 2001). The system is calibrated using the mass spectrometer signal from a sample of known vapour pressure, in this case malonic acid (vapour pressure at 298K = 5.25×10^{-4} Pa, (Booth *et al.*, 2012)). A load-lock allows the ioniser filament to be left on, then a new sample of unknown vapour pressure can be measured. Solid state vapour pressures measured in the KEMS can then be converted to sub-cooled liquid vapour pressures using the melting point, enthalpy and entropy of fusion, which are obtained by using a Differential Scanning Calorimeter (DSC) (TA instruments Q200).~~

~~2.6~~ SCO ~~identification~~Measurement

~~Peak fitting was performed utilizing the Tofware peak fitting software for molecular weights up 620 AMU. Unknown peaks were added to each peak~~

2.5.1 Identification

Spectral analysis was performed using Towfware V2.5.11. the average peak shape for the tuning utilised for this campaign was used to calculate the mass resolution and optimization of the baseline fit. The mass spectrum was mass calibrated (allowing for accurate centroid peak position to be estimated, improving on a Gaussian assumption) using 4 ions up to mass 527 (the dimer of perfluorpentanoic acid) and applying a custom peak shape to achieve accurately peak identification below 5 ppm error across the mass range (0-620 AMU). A time series of the mass calibrant error for the entire campaign (figure SI1) illustrates how the error deviated by only +/-1 throughout the measurement period. This provides confidence that variation in signal and peak positioning did not result in large errors of identification and quantification of the analyzed peaks. *A priori* unknown peaks were added to resolve overlapping peaks on the spectra until the residual was less than 5%. Each unknown peak was assigned a chemical formula using the peaks exact mass maxima to 5 decimal places and also isotopic ratios of subsequent minor peaks. An accurate fitting was characterized by a ppm error of less than 5 and subsequent accurate fitting of isotopic peaks. An example of the spectra and peak fitting can be found in Figure 1, highlighting the mass spectral fit for GAS and ~~nitrophenol sulfate (NP OS), previously identified ambient SCOs.~~$C_9H_9SO_5$.. Although the structure cannot be determined with CIMS, it is assumed that no fragmentation of larger SCO species contribute to the SCO identified due to the soft ionization technique employed. The SCOs were identified in the spectra as negative ions assumed to be formed by hydrogen removal. Here, we present 17 SCOs that were identified in the mass spectra, which are displayed in Table 1 with their respective exact mass, formula, literature nomenclature and possible precursors. The peak fittings for all 17 SCOs is presented in the supplementary (SI2). All 17 SCOs represented a significant signal in the average desorption spectra from the particle phase analysis. It must be noted that gas phase spectra at times contained other ions at a similar mass to the SCOs that contributed to higher counts than the SCO. This may result in a variable error to the measurement, although this should be at a minimum due to the use of a custom peak shape and low general mass calibration error of the spectra. The SCOs detected ions ranged from 154.96 *m/z* (GAS) to 294.06 *m/z* ($C_{10}H_{11}NSO_7$). The number of oxygen in the SCO ranged from O_3 ($C_7H_7SO_3$) to O_7 ($C_5H_8SO_7$). ~~Filter measurements were taken diurnally at the same sampling site, although from a different inlet and location in the building, to which orbitrap and HPLC MS analysis was performed to identify OSs present in the ambient air. The CIMS measurements generally agreed well, once processed into diurnal loadings, which confirms the correct identification and measurement of SCOs by CIMS. This analysis is not within the scope of this work and provides the basis of the correct identification to which a future paper will probe the caveats observed between the measurement techniques.~~

It is acknowledged that the CIMS may not detect all SCOs in the ambient air due to peak fitting resolution limitations and limits of detection, therefore enabling the possibility for misrepresentation of the dominant SCO and an underestimation of total abundance~~, although for the analysis in this work it is assumed that the measured SCOs do represent a significant fraction. No~~. However, no physical features of the SCO (structure, O:C ratio, mass etc.) should inhibit the CIMS identifying the major SCO in the Beijing ambient air. Consequently, we here, and to facilitate descriptions of the relationship between individual SCOs and the total SCO measure, assumed that the measured SCOs do represent a significant fraction.

Formatted: Indent: Left: 0 cm

2.~~7~~5.2 Quantification of SCOs

The OS and NOS calibrations ~~were performed after the campaign and~~ normalized to~~ the in situ~~ formic acid calibrations (as described in le Breton *et al*., 2012, 2013) to account for any drift in sensitivity throughout the campaign. This relative sensitivity technique has been previously utilized for N_2O_5 and $ClNO_2$ and has been verified with laboratory experiments (Le Breton *et al*., 2014). As a result of low mass range of the SCOs, common functionality, relatively small change in polarity and lack of available stable SCO standards, we calibrated for 2 SCOs (lactic acid sulfate (LAS) and NP OS) and applied an average sensitivity for all the SCOs detected in Beijing. The ToF-CIMS sensitivity utilizing iodide as a reagent ion is known to vary by up to 3 orders of magnitude; therefore, further work is necessary to develop SCO standards and assess possible variations in sensitivity. NP OS is available commercially from Sigma Aldrich and was utilised to calibrate for the NOS's. L(+) Lactic acid from Sigma Aldrich (95%) was utilised as the preliminary agent for lactic acid sulfate synthesis and was produced using the same technique as Olson *et al*. (2011). Briefly, a solution of 76.1 mg, 1.29 mmol, lactic acid in 2 mL di-methyl-formamide (DMF) was added dropwise to sulphur trioxide pyridine (0.96g, 7.75mmol) in 2mL DMF at 0 ^{o}C. The solution is then stirred for 1 hour at 0 ^{o}C and 40 minutes at room temperature, the solution is re-cooled to 0 ^{o}C and trimethylamine

(0.23 mL, 1.66 mmol) was added for quenching and the mixture wad further stirred for 1 hour. The solvent is then evaporated under vacuum and NMR is directly utilised to calculate the purity which was found to be 8.2%.

A known mass of the solid calibrant (NP OS and Lactic acid sulfate) was added to 3 different volumes of milliQ water to produce different concentration standards. A known volume of each solution was then placed onto the FIGAERO filter and a desorption cycle was performed. The total ion counts for the HR SCO peak relates directly to the sensitivity of the system with respect to total ion counts per molecule reaching the detector. Figure 2 shows a 3-point calibration curve for NP OS and the corresponding thermogram, mass spectra and peak fit. The sensitivity of LAS and NP OS calibrations were calculated to be 2.0 and 1.6 ion counts per ppt Hz^{-1} respectively. All SCO were calibrated using the LAS sensitivity and all NOS using the NP OS sensitivity.

During desorption of both SCOs, fragmentation of the organic core and sulphate group was observed resulting in a desorption profile ~~of~~ at *m/z* 97 (the bisulphate ion) and the deprotonated organic mass, i.e. $C_3H_5O_3$ for lactic acid. A number of different temperature ramping rates were performed with the FIGAERO to further probe the fragmentation and highlighted an increase in ramp rate (^{o}C/minute) decreased the calculated sensitivity due to an increase in fragmentation. This not only serves to highlight how the calibration tests of a species must mimic the exact measurement conditions, but also suggests potential interferences from fragmentation on the organic *m/z*´s. The relatively low concentration of the ~~OS~~organic precursor with respect to the ~~organic precursor~~SCO results in little error in quantification, although this ratio may significantly change in different air masses and a number of products of organic oxidation may fragment resulting in a significant error. This fragmentation can also be observed within the high resolution thermograms of the FIGAERO as a double desorption and further highlights the necessity for detailed thermogram analysis to accurately deconvolve desorption's relevant only to particle loss from the filter and not fragmentation or ion chemistry in the IMR. The fragmentation is considered to be constant throughout the campaign. The error for the SCO measurements ~~will~~may vary for each individual ~~OS.~~SCO possibly due to structure, volatility and fragmentation. It is commonly accepted within the literature for compounds lacking calibration that a functional group sensitivity can be applied (e.g. Lee *et al*., (2016) for ONs). Here we calculate an average error of 52 % for the SCOs, calculated using the standard deviation of the NP OS calibration time series data.

The limitation of FIGAERO temperature ramps to 250 ˚C may result in further error as some SCOs may not be fully desorbed from the filter due to their low vapour pressures. To evaluate the mass left on a filter, several double desorption cycles were performed where mass is collected and desorbed such as in standard use. This is performed by re-heating the same filter once cooled to attain a second thermogram of the same filter. The second thermogram exhibited an average of 90% reduction of counts for the ~~OS~~SCO, although the NOSs had an average decrease of 82% counts. This indicates that most, but not all mass, are removed from the filters when desorbing. For the interpretation of the results of the field campaign this effect will induce a small distortion on the time evolution of SCOs when comparing to other parameters, e.g. 9% of NOSs will remain on the filter and being subjected to the subsequent desorption cycle.

2.5.3 Offline and online measurement comparison of SCOs

Filter measurements, for orbitrap and HPLC MS analysis, were taken diurnally at the same sampling site, although from a different inlet and location in the building. The CIMS hourly desorption data was averaged over corresponding collection period to attain a day and nighttime CIMS data point. The period between the 23rd May and 1st June was selected due to all instrument measurements being undisturbed during this period. It must be noted that CIMS data is lacking one data point daily while the background filter measurements were taken. The CIMS, orbitrap and HPLC do not measure all of the same species. Here a comparison of total 5 ions is presented with the HPLC and 2 from the orbitrap, where a further extensive comparison is to be performed in an accompanying manuscript. Figure SI3 illustrates the time series of CIMS (hourly and diurnal) measurements of GAS and IEPOX sulfate alongside the HPLC measurements. The diurnal data agrees well with an R value of 0.78 and 0.82 for GAS and IEPOX sulfate respectively. The sum of the time series we have multi instrument data for (GAS; IEPOX sulfate, LAS, $C_4H_7SO_7$, $C_5H_{11}SO_7$ and $C_5H_7SO_7$) for HPLC and $C_9H_{11}SO_5$ and $C_9H_8SO_5$ for orbitrap is displayed in the top panel. In general, the time series agree well and also have a good correlation (R = 0.7 and 0.81 for HPLC and orbitrap respectively) illustrating the ability for CIMS to agree with the offline methods and measure the SCOs accurately at low and high time resolution.

2.7 Knudsen Effusion Mass Spectrometer (KEMS)

The KEMS technique was utilized to measure the vapour pressure of SCOs observed in the gas phase measurements by the CIMS. The KEMS technique is able to measure vapour pressures from 10^{-1} to 10^{-8} Pascals (Pa) ranging from volatile organic compounds to extremely low volatility organic compounds. A full description of the technique can be found in Booth *et al*. (2009, 2010) and the measurements of a series of compounds over a large VP range, in a recent inter-comparison study from this instrument, can be found in Krieger *et al*. (2017). Briefly, the instrument consists of a temperature controlled Knudsen effusion cell, suitable for controlled generation of a molecular beam of the sample organic compounds in a vacuum chamber, coupled to a quadrupole mass spectrometer. The cell has a chamfered effusing orifice with a size <1/10 the mean free path of the gas molecules in the cell. This ensures the orifice does not significantly disturb the thermodynamic equilibrium of the samples in the cell (Hilpert, 2001). The system is calibrated using the mass spectrometer signal from a sample of known vapour pressure, in this case malonic acid (vapour pressure at 298K = 5.25×10^{-4} Pa, (Booth *et al*., 2012)). A load-lock allows the ioniser filament to be left on, then a new sample of unknown vapour pressure can be measured. Solid state vapour pressures measured in the KEMS can then be converted to sub-cooled liquid vapour pressures using the melting point, enthalpy and entropy of fusion, which are obtained by using a Differential Scanning Calorimeter (DSC) (TA instruments Q200).

3. Concentrations and partitioning of atmospheric SCOs

3.1 SCO contribution to PM$_1$ at Changping

The SCOs measured at the Changping site had a mean campaign concentration of ~~207± 106~~210+ 110 ng m^{-3} (Table ~~2~~1). The highest concentration of total SCOs during the campaign was ~~542~~540 ng m^{-3} and the lowest 40 ng m^{-3}, thus they are omnipresent and have significant sources during most atmospheric conditions. These concentrations are consistent with Stone *et al*. (2012) reporting an average ~~OS~~SCO concentration of 700 ng m^{-3} in a number of rural and urban sites in Asia. A mean SCO contribution to OA in the work presented here was calculated to be 2 ~~± 2.8~~.0 ± 1% (Table ~~2~~1), within the range of values calculated by Stone *et al.* (2012) (0.8% to 4.5%), further supporting evidence that SCO contribution to PM$_1$ mass is relatively low in Asia. The CIMS cannot claim to measure total SCO, rather than singularly identify and measure SCOs contributing to the total mass loading. Therefore, the SCO contribution reported in this work should be considered as a lower limit. The Liao *et al*. (2015) study also supports the idea that SCO contribution to PM$_1$ mass in anthropogenically dominated regions is less significant than that from biogenically dominating air masses by observing a significantly higher contribution of IEPOX sulfate to PM$_1$ mass on the East coast of the United States (1.4%) than the West Coast (0.2%).

The observation of higher relative contribution of SCOs to total organics in more remote regions compared to a densely populated urban area, supports the idea that SCOs provide a higher contribution to ~~mass~~PM in aged air due to their secondary production pathways. Similar to Lahore (as studied by Stone *et al*., 2012), Beijing has many strong primary anthropogenic sources which will dominate the mass loading and therefore, initially, will contribute to a lower fraction of the total concentration from ~~SOA~~secondary production due to limited processing near the source. Throughout the campaign, a good correlation (R^2 = 0.66) was observed between an increase in ΔSCO mass and PM$_1$ mass, although the ~~OS~~SCO contribution to PM$_1$ decreased exponentially (Figure 3) indicating that the pollution episodes contain a lower fraction of SCOs with respect to total PM$_1$ ~~than the clean air days and that high pollution containing air masses contained more OSs but at a less significant fraction. This reuslt also suggests trhat~~. This result suggests that SCO do not play as large a role as expected even though their precursors (organics and sulfate) ~~ar~~are abundant within the episodes, indicating the conditions of their formation may be more vital than absolute concentrations of precursors.

3.2 Gas to particle phase partitioning of SCOs

The FIGAERO ToF-CIMS data exhibited indication of SCOs in both the particle and gas phase. Previous studies have supported the existence of e.g. gas phase GAS in ambient air (e.g. Ehn *et al*., 2010), although some work has attributed other measurement techniques detection of gas phase SCO to result from measurement artefacts (Hettiyadura *et al*., 2017; Kristensen *et al*., 2016). Once all HR peaks have been identified, the batch fitting and HR time series for the whole data set is processed and then separated into gas phase measurements and particle phase desorption profile time series. ~~Subtraction~~The data is background corrected i.e., subtraction of both the gas phase background periods and blank filter desorption's~~ removes any data underneath the detection threshold of ambient gas species and particles~~. Upon analysis of the resultant data, significant concentrations of gas phase SCOs were observed. Figure 4 depicts the overall sum SCO mass concentration time series in the gas and particle phase. The mean contribution from gas phase SCO to total SCO was found to be 11.6%, 23±8 ng m^{-3}. This suggests a significant amount of ~~OS~~SCO is always present in the gas phase and factors that influence gas-to-particle partitioning ~~sustain~~ influence the level of this ~~significant~~ contribution. ~~The R^2 correlation between gas phase and particle phase SCOs is 0.43 that suggests reliability upon total SCO for partitioning but indicates a more complex system that governs the partitioning. This low correlation~~These changes in contribution also ~~further supports~~reduce the ~~probability that the concentrations do not results from an instrument artefact as this would likely to result in a constant ratio of particle to gas phase concentrations. Previous studies have supported the existence of gas phase GAS in ambient air (~~possibilities for memory effect , e.g. one~~Ehn *et al*., 2010), although some work has attributed other measurement techniques detection of gas phase SCO to result from measurement artefacts (Hettiyadura *et al*., 2017; Kristensen *et al*., 2016). One~~ possibility is the deposition of SCOs onto the IMR walls during the temperature ramp of the desorption which in time may de-gas and be observed in the gas phase. This would likely ~~to~~result in a constant ratio of particle to gas phase concentrations and would likely cause a hysteresis in the observed gas phase measurements with respect to the particle phase, which was not observed.

The vapour pressure of NP OS was measured using the KEMS instrument in the laboratory to establish the ~~possible~~ existence of gas phase SCOs. This technique has recently been employed to measure the vapour pressure of NP (Bannan *et al*., 2017). The KEMS experiments found the solid state vapour pressure of NP OS to be 5.07×10^{-5} Pa at 298 K. Assuming an average subcooled liquid correction for all compounds measured in the Bannan *et al*. (2017) study, as no DSC data is available, the subcooled liquid vapour pressure of NP OS is 2.32x10^{-4} (Pa). This vapour pressure lies within the semi volatile organic compound range, therefore supporting the potential partitioning of ~~OSs~~SCOs to the gas phase under ambient conditions. ~~Analysis of each OS T$_{max}$ from the FIGAERO indicates that more than half of the SCOs detected have a higher vapour pressure than NP OS which also indicates a significant partitioning towards the gas phase. This is an unexpected result due to the lack of literature indicating OSs have a gas~~

~~phase presence.~~ To further validate the CIMS and KEMS findings, one can ~~further calculate the~~ evaluate different compounds VPs from the FIGAERO data utilizing the T_{max} and compare ~~these~~ to literature values~~, confirming that the partitioning calculated by CIMS is representative for compounds well established within the literature.~~. The CIMS ~~calculated~~, using T_{max}, estimated VPs of malonic, succinic and glutaric acid ~~were~~to be $2x10^{-3}$, $1.85x10^{-3}$, $1x10^{-3}$ Pa which compare well to ~~the~~ values presented by Bilde *et al*. (2015) VPs; $6.2x10^{-3}$, $1.3x10^{-3}$, $1x10^{-3}$. ~~This~~Using this agreement ~~further supports the NP OS KEMS VP and therefore the partitioning~~ for well-known substances we notice the T_{max} of SCO to be in the range were it can provide significant gas-phase concentration. Still, the observed presence of gas phase GAS and IEPOX-OS does not agree with previous studies of these compounds (Stone *et al.*, 2012, Hettiyadura *et al.*, 2017). Therefore, one need to be cautious and deeper analysis into exact VPs and partitioning from the present work must be performed to assess whether their gas phase presence could be fully confirmed. So far we note that fragmentation of organic species (oligomers) during desorption could lead to a potential artefact and a lower T_{max} at a monomer peak (Stark *et al*., 2017 and Lopez-Hilfiker *et al*., 2016). However, here we identify and expect no dimers or oligomers that could fragment to form the SCOs identified. Furthermore, the higher mass organics are likely to have a much higher VP than the lower mass SCO and provide a second T_{max} which would produce a lower VP value due to the greater energy required to break the bonds. Analysis of T_{max} throughout the campaign shows no double peak thermograms and an acceptable stability of T_{max}(SI4). T_{max} varied by ~~CIMS for uncalibrated OSs. Aerosol~~up to 14 Celisus and appeared to correlate well with particulate loading, similar to that observed by Huang *et* al., (2017), who suggested that this is a result of diffusion limitations within the particle matrix. If the data is tentatively analyzed to assess mechanism regarding their partitioning, aerosol liquid water content ~~will~~would affect the partitioning of gas phase compounds to aerosols (Zhang *et al*., 2007). Data point size coding the correlation of the gas and particle phase SCO concentrations indicates partitioning towards the aerosol phase at lower relative humidities (Figure 4). Conversely, as temperature increases (as indicated by red colour shading) the SCOs partition further towards the gas phase, as thermodynamically expected.

~~NOS $C_{10}H_{16}NO_7S$ displayed the highest particle to gas phase ratio of 13.9 and has mean presence in the gas phase of 4.4%. The most prominent gas phase SCO particle to gas phase ratio was IEPOX OS which has a particle to gas phase mean ratio of 1, indicating, on average, this SCO is evenly distributed between the gas and particle phase. GAS, as measured in the gas phase in previous literature (Ehn *et al.*, 2010) has a mean particle to gas phase ratio of 10.3, contributing to 7.1% of GAS from the gas phase with a maximum campaign contribution in the gas phase of 29.5%.~~ Further work is necessary to validate these findings and determine the mechanisms and importance of gas phase SCO abundance in ambient air. ~~The significant contribution of IEPOX-sulfate in~~For example, the ~~gas phase is an unexpected result, which could have serious implications on our knowledge of SOA formation. One possible, explanation is a gas phase formation pathway of IEPOX sulfate. The~~ high contribution in the gas phase could ~~also~~ be ~~further~~ perturbed if ~~an~~ equilibrium between condensation to particle phase and gas phase formation has not been established. It must be noted that the ~~VP of these compounds has not been calculated and~~a correct calibration of T_{max}

~~is~~ with VP would be, necessary to extract such information, but qualitatively the relative VP compared to NP OS ~~can~~could be utilized as a reliable scale due its independent calibration by KEMS.

Formatted: English (U.S.)

4. Sources and secondary formation of SCOs

4.1 SCO sources at the Changping site

SCOs are known to have biogenic and anthropogenic sources and some which have multiple sources from both, e.g. GAS (Hettiyadura *et al.*, 2017; Hansen *et al*., 2014). Burning events are known to emit high levels of organics and nitrates and potentially sulfur, depending on the type of fuel used. This enables biomass burning to be a potential anthropogenic and biogenic source of SCOs~~ through release of their precursors.~~. The site at Changping was influenced by both regional anthropogenic pollution from the Beijing area and localized anthropogenic activity (industry, biomass burning and traffic) but also emissions from biogenic sources, as it is situated in a semi-rural area, with forest, vegetation and plantations. This was evident from the ~~toluene~~benzene and isoprene ~~proton transfer mass spectrometer (~~PTR-MS~~)~~ measurements which have mean campaign concentrations of 0.55 ± 0.4 and 0.27 ± 0.19 ppb respectively with maxima of 5 and 1.5 ppb respectively. Thus, as shown in Figure 5, PTR-MS measurements ~~of benzene and isoprene~~ mean daily concentrations were utilized to evaluate ~~and exemplify~~if the ~~attribution of~~ ratio benzene and isoprene can indicate a higher mass loading and contribution of aromatic and biogenic ~~mass contribution of~~ SCOs measured in this work. Data on days with incomplete time series have been removed to ensure the data presented represents a full mean of the day concentration. A good correlation between the benzene:isoprene ratio and sum of SCOs is observed. It suggests an increase in relative anthropogenic emissions promotes an increase in total SCO loading. It should be noted that $C_6H_{10}SO_7$ has no known precursor in the literature, although it contributes significantly to the SCO mass loading in this work (16%).

4.1.1 *Biogenic and anthropogenic SCOs*

Biogenic SCOs are known to be comprised of monoterpene, sesquiterpene and isoprene derived SCOs which have been identified in rural, sub-urban and urban areas around the world, and have been shown to be a major constituent of SOA (Surratt *et al*., 2008; Shalamzari *et* al., 2014, Liao *et al*., *2015*). IEPOX sulfate is commonly found to be the most dominant ~~OS~~SCO at many locations and was identified ~~in the spectra~~also at the Changping site. The IEPOX sulfate mean concentration represented 0.11% of the OA mass, agreeing well with concentrations found in Western USA (significant anthropogenic emissions) and lower than the Eastern USA as expected due to higher biogenic and isoprene emissions (Liao *et al.*, 2015). Although IEPOX sulfate is considered one of the most abundant individual organic molecules in aerosols (Chan *et al*., 2010), here our results show it only contributed to 2% of the SCO mass and was the 8th most abundant SCO in the particle phase. Additionally, two other isoprene derived SCOs, $C_5H_8SO_7$ and $C_4H_8SO_7$, were~~ also two isoprene derived OSs~~ measured by the CIMS with mean campaign concentrations of 2 and 3 ng m^{-3} respectively and a contribution of 0.02% to OA mass. The highest contributing biogenic SCO to the ambient air was a NOS, $C_{10}H_{16}NSO_7$, a known NOS derived from alpha-pinene oxidation. This NOS had a mean campaign concentration of 21 ng m^{-3} and a 0.2% contribution to OA mass.

Anthropogenic SCOs, including polyaromatic hydrocarbon (PAH) derived SCOs have received more attention in ~~research~~recent studies due to their identification ~~and therefore can also contribute to altering SOA hygroscopicity and radiative properties via acting as surface reactants~~ (Nozière *et al*., 2010; Hansen *et al*., 2015). Aromatic SCOs and sulfonates have only recently been identified as atmospherically abundant SCOs (Riva *et al.*, 2015). In this work we find that the PAH derived SCO $C_{11}H_{11}SO_7$ is the most dominant SCO in Beijing with a mean concentration of 40 ng m^{-3}, contributing to 20% of the total SCO mass and 0.4% of the OA mass. This SCO has been identified in laboratory studies as an SCO forming from the photo-oxidation of 2-methyl napthalene, one of the most abundant gas phase PAHs and is thought to represent a missing source of urban SOA (Riva *et al.*, 2015). This work presents the possible significance of PAH SCOs in Beijing and further evidence that photo-oxidation of PAHs represents a greater SOA potential than currently recognized. A further 8 anthropogenic aromatic derived SCOs were identified as common components of the PM_1 representing more than half of the total SCOs with $C_7H_5SO_4$ contributing to 24 ng m^{-3} and 0.23% OA mass. The total anthropogenic related SCOs had a mean mass of ~~122~~120 ng m^{-3} and contributed to 1.2% of the OA mass.

4.1.2 *Biomass burning source of SCOs*

NP (a product of benzene oxidation and nitration) has previously been detected in the gas and aerosol phase (Harrison *et al.*, 2005) and is an important component of brown carbon (Mohr *et al.*, 2013). NP has primary sources, such as vehicle exhausts and biomass burning (Inomata *et al.*, 2013 and Mohr *et al.*, 2013) and secondary sources via the photo-oxidation of aromatic hydrocarbons in the atmosphere (Harrison *et al.*, 2005). High levels on anthropogenic activity, biomass burning and strong photochemistry in Beijing therefore enable this region to be a strong potential source of NP. ~~Diurnal profiles of NP exhibit a significant increase in the morning, possibly due to both local biomass burning and vehicle emissions, which is maintained throughout the day. A second large increase in concentration is observed around 4pm, likely due to vehicle activity. The NP OS also exhibits a similar diurnal structure, although its concentration builds up more rapidly in the afternoon and early evening, likely to be a result of the photochemical aging of NP and eventual reaction with SO_4^{2-} to produce the OS.~~Both NP and NP OS diurnal profiles exhibit an increase in the morning (6am onwards) although NP OS appears to increase in concentration more rapidly. The early morning biomass burning and anthropogenic activity are likely to contribute to production of both species, although the higher sulphate content of the biomass burning emissions may promote a faster production of NP OS and conversion of NP to NP OS. Both compounds continue to increase with a photochemical profile with one peak at midday but also a peak around 4pm, likely to be a second source of the day from anthropogenic activity. The NP OS continues to increase until sunset, which could result from further photochemical production from the NP emitted throughout the day whereas NP falls off after the 4pm peak. The campaign time series for NP and NP OS can be seen in Figure 6. Unlike its precursor and most other pollutant markers measured in this work, including all other ~~SOCs~~SCOs, NP OS exhibits higher concentrations between ~~28th~~17th to the ~~1st June~~22nd May compared to the ~~17th~~28th May to ~~21st May~~3rd June. The only compound with a similar campaign profile is acetonitrile (a marker for biomass burning), which has significantly enhanced concentrations between 6 and 8am from the 17th to the ~~21st~~22nd May. Back trajectories of these two time periods show the air mass during the first period comes from the west, a more rural region of China and known to be influenced heavily by biomass burning, whereas the second time period has wind directions mainly bringing in air masses that have gone through the Tianjin and Beijing area. It is therefore hypothesized that the NP OS, which peaks later in the day than the NP and acetonitrile, is a secondary product formed from the biomass burning ~~events indicated by the acetonitrile data~~and has aged after being emitted from air masses further away. Here NP can have more local sources of biomass burning and traffic which then can contribute to NP OS production, but at a slower time scale, which in this data set, appears as lower production due to the limited oxidation of local air masses.

4.2 SCO production mechanisms

4.2.1 *Precursor analysis*

The availability of the organic precursors of SCOs is a limiting factor for the SCO production rate. The measurement of the precursors in the gas and particle phase by CIMS enables a more descriptive mechanism to be outlined as the partitioning of the precursor will vary the distribution between gas and particle production pathways and therefore rate of corresponding SCO production. Glycolic acid has on average 75% of its mass in the gas phase for the measurement period whereas GAS is dominantly in the particle phase (Figure 7). The GAS particle phase concentration is observed to increase as the SO_4^{2-} mass loading increases and the GA gas and particle concentrations increase, although the partitioning of the GA towards the gas phase restricts the ~~OS~~SCO production. This can be seen in Figure 7 as for a given SO_4^{2-} concentrations, the data with warm colors (red), representing high fraction of precursor GA in particle phase, generally provides higher concentration of particulate GAS.

The main formation mechanism of GAS is thought to be via the reaction of GA in the gas phase with an acidic aerosol sulfate (Liao *et al.*, 2016), contrary to what is observed here. Although an increase in GAS is observed to correlate with the GA, it appears that a partitioning towards the particle phase promotes GAS production. An R^2 correlation of 0.68 between GAp and GASp whereas an R^2 of 0.4 is observed between GAg and GASp.

The sum of benzene SCOs exhibits a good correlation to the gas phase benzene time series (Figure 8), although their abundance should also rely on the availability of sulfur in the particle phase and the age of the air mass, if it is assumed that they are formed via secondary reactions of primary pollutants. In order to assess how the SCO production rates may vary due to these factors, two distinct high benzene SCO events with similar benzene concentrations were scrutinized, i.e. the 29th May and the 1st June. The first period has lower SO_4^{2-} concentrations, higher H_2SO_4 levels and a higher total benzene SCO concentration. The exact age (or time for oxidation) of compounds in an air mass are without an extensive modelling study complicated to derive. However, as proxies to attain an approximation about oxidation state one may use some trace compounds. Monoterpene oxidation by the hydroxyl radical (OH) or O_3 results in the formation of multifunctional organic acids such as pinonic acid which can then be further oxidised by OH to form 3-methyl-1,2,3-butane-tricarboxylic acid (MBTCA), both of which are measured by CIMS. Therefore, in an air mass containing monoterpene emissions, as known here through the identification of their products such as $C_{10}H_{16}NO_7S$, we can utilize the ratio of pinonic acid and MBTCA; as tracers of monoterpene SOA processing as detected in ambient aerosols in Europe, USA and Amazon (Gao *et al*., 2006) as a relative photochemical clock. During the high benzene event on the 1st June, according to the pinonic acid: MBTCA ratio, the air mass is less oxidized relative to the air mass on the 29th May (Figure 8). This would allow less time for secondary production and explain the relatively lower concentration of SCOs, irrespective of higher SO_4^{2-} concentrations and similar benzene concentrations.

To further elaborate The Gothenburg Potential Aerosol Mass (Go:PAM) ~~chamber~~reactor (Watne et al, 2018) was tested and utilized to simulate aging of the air mass during periods of the campaign. Here the ratio between pinonic acid and MBTCA was observed to increase by an average of 3 during aging within the Go:PAM which has been calculated to be the OH exposure equivalent of 2 days in the ambient atmosphere. As this ratio increased with aging, the SCO concentration also increased exponentially, further supporting the secondary production of SCO in photochemically aged air mass. Although limited data is available here for simultaneous Go:PAM and CIMS measurements, the results indicate the potential utilization of the chamber to probe secondary production processes.

4.2.2 *Aerosol acidity*

The molecular ion $H_3S_2O_7^-$ was identified in the mass spectra throughout the campaign, which has previously been detected by Liao *et al*. (2015) using a Particle Analysis Laser Mass Spectrometer to measure SCOs. They attribute this mass to be a cluster of HSO_4^- with sulfuric acid (H_2SO_4). Particles in the presence of H_2SO_4, and therefore high acidity, form this cluster whereas neutralized ions are likely to favour the unclustered HSO_4^- form. Therefore, the ratio between the cluster and the bisulfate ion increases with increasing aerosol acidity (Murphy *et al*., 2007; Carn *et al*., 2011). Liao *et al*. (2015) validate the appropriateness of this cluster as a marker for aerosol acidity thorough comparisons to a thermodynamic model with gas and aerosol phase measurement inputs. Acidity was also calculated utilizing the gas and particle phase H_2SO_4 and liquid H^+ ion concentration analysed using an offline technique, as described by Guo *et al.* (2010), from diurnal samples taken at the site. This method showed good agreement with the integrated diurnal counts of the $H_3S_2O_7^-$ ion~~ and therefore.~~. Therefore, we employ the $HSO_4^-.H_2SO_4^-$ cluster in this work as a qualitative scale for particle acidity utilizing similar assumptions. Figure 9 shows how total SCO mass concentration generally increased as total organic mass from the AMS increased. The correlation indicates that higher acidity (darker colours) tends to promote formation of SCOs when in the presence of high levels of organics and SO_4^{2-} (larger symbol sizes), supporting the growing consensus that aerosol acidity plays an important role in ambient SCO formation. This importance of acidity agrees well with both the acid-catalyzed epoxydiol ring opening formation mechanism (Surratt *et al*., 2010) and the sulfate radical initiated SCO formation because efficient formation of sulfate radicals also requires acidity (Schindelka *et al*., 2013).

5. Conclusions

The FIGAERO ToF-CIMS was successfully utilized for the ambient detection of 17 SCOs in Beijing in the gas and aerosol phase with limits of detection in the ng m^3 range. Good agreement with offline filter measurements further supports the robustness of this method for high and low time resolution measurements of SCOs. Further calibrations and comparisons to total SCO measurements are required to evaluate its performance limitation with regards to sensitivity application and peak identification. The SCOs measured by CIMS contributed to 2% of the OA at the semi-rural site, highlighting the relatively low contribution of SCOs in Beijing, an anthropogenically dominated environment. This calculation from CIMS may only be valid to infer each individual SCO contribution to total SOC mass as limitations in SCO identification and quantification limit the CIMS ability for total SCO measurements. Significance of their secondary production pathway prevailed, although still present in relatively fresh air masses. Contributions of SCO to total organics (2~~±2.8~~.0±1%), sulfate (15±19%) and PM (1.0±1.4%) indicate the concentrations observed~~ emissions~~ in Beijing result from highly processed ambient air masses.

Gas phase SCOs were identified for all the SCOs measured at the site, contributing to in average to ~~18~~12% of the total SCO mass. The possibility of gas phase ~~OSs~~SCOs in ambient air was supported by KEMS vapour pressure measurements of NP OS and derived T_{max} values which ~~suggests~~suggest a vapour pressure in the semi volatile range. ~~A number of SCOs possessed T_{max} values similar to that of NP OS indicating they should also have semi volatile vapour pressures which is indicated by their gas phase presence observed in this work.~~ The partitioning towards the gas phase was more efficient at high atmospheric temperatures, while lower relative humidities promoted partitioning to the particle phase.

Biogenic SCOs contributed to a small fraction of the total ~~OS~~SCO mass at Changping and was dominated by an ~~alpha~~ α-pinene derived OS with 0.2% contribution to the OA mass. IEPOX sulfate was only the 8th most abundant SCO measured, contrary to common reports that it is one of the most abundant ~~OS within the aerosol.~~SCO. Anthropogenic precursors contributed to more than half of the SCO mass loading with a PAH derived SCO contributing to as much as 1.2% of the OA mass. Benzene derived SCOs correlated well with gas phase benzene levels and were heavily influenced by photochemical aging~~, as indicated by the pinonic acid: MBTCA ratio.~~. The contribution of each benzene derived SCO to total benzene derived SCO mass varied daily and throughout the campaign highlighting the complexity of the atmospheric processing and composition of ~~SC~~SCO. Significant contributions from aromatic SCOs highlight the importance of anthropogenically emitted organics in the Beijing region and their contribution to the Beijing outflow and subsequent photochemistry. NP OS was attributed to biomass burning emissions due to ~~its campaign intensity coinciding~~co-occurrence with high levels of acetonitrile. This highlights the importance of anthropogenic emissions and their contribution to SOA from the urban Beijing outflow.

A qualitative CIMS marker for aerosol acidity highlighted the increase in SCO production rate in acidic aerosols in the presence of high SO_4^{2-} and organics. The correlation of SCO production and RH becomes more complex for individual SCOs, which cannot be resolved within this studies framework.

Formatted: Font: Bold

Acknowledgement:

The work was done under the framework research program on ‘Photochemical smog in China” financed by Swedish Research Council (639-2013-6917). The National Natural Science Foundation of China (21677002) and the National Key Research and Development Program of China (2016YFC0202003) also helped fund this work.

References

Bannan, T. J., Booth, A. M., Jones, B. T., O’Meara, S., Barley, M. H., Riipinen, I., Percival, C. J., and Topping, D.: Measured saturation vapor pressures of phenolic and nitro-aromatic compounds, Environ. Sci. Technol., 51 (7), 3922–3928, 2017.

Booth, A. M., Markus, T., McFiggans, G., Percival, C. J., Mcgillen, M. R., and Topping, D. O.: Design and construction of a simple Knudsen Effusion Mass Spectrometer (KEMS) system for vapour pressure measurements of low volatility organics, Atmos. Meas. Tech., 2, 355–361, 2009.

Booth, A. M., Barley, M. H., Topping, D. O., McFiggans, G., Garforth, A., and Percival, C. J.: Solid state and sub-cooled liquid vapour pressures of substituted dicarboxylic acids using Knudsen Effusion Mass Spectrometry (KEMS) and Differential Scanning Calorimetry, Atmos. Chem. Phys., 10, 4879–4892, 2010.

Booth, A. M., Bannan, T., Barley, M. H., Topping, D. O., McFiggans, G., and Percival, C. J.: The role of ortho, meta, para isomerism in measured solid state and derived sub-cooled liquid vapour pressures of substituted benzoic acids, Roy. Soc. Chem., 2, 4430-4443, 2012.

Boris, A. J., Lee, T., Park, T., Choi, J., Seo, S. J., and Collet Jr, J. L.: Fog composition at Baengnyeong Island in the eastern Yellow Sea: detecting markers of aqueous atmospheric oxidations, Atmos. Chem. Phys., 16, 437-453, 2016.

Bruggemann, M., Poulain, L., Held, A., Stelzer, T., Zuth, C., Richters, S., Mutzel, A., van Pinxteren, D., Iinuma, Y., Katkevica, S., Rabe, R., Herrmann., and Hoffmann, T.: Real-time detection of highly oxidized organosulfates and BSOA marker compounds during the F-BEACh 2014 field study, Atmos. Chem. Phys., 17, 1453–1469, 2017.

Carn, S. A, Froyd, K. D., Anderson, B. E., Wennberg,P., Crounse, J., Spencer, K., Dibb, J. E., Krotkov, N. A., Browell, E. V., Hair, J. W., Diskin, G., Sachse, G., and Vay, S.: A. In situ measurements of tropospheric volcanic plumes in Ecuador and Colombia during TC4, J. Geophys. Res., 116, D00J24, 2011.

Chan, M. N., Surratt, J. D., Claevs, M., Edgerton, E. S., Tanner, R. L., Shaw, S. L., Zheng, M., Knipping, E. M., Eddingsaas, N. C., Wennberg, P. O., and Seinfeld, J. H.: Characterization and quantification of isoprene-derived epoxydiols in ambient aerosol in the Southeastern United States, Environ. Sci. Technol., 44,12, 4590–4596, 2010.

de Gouw, J. and Warneke, C.: Measurements of volatile organic compounds in the earths atmosphere using proton-transferreaction mass spectrometry, Mass Spectrom. Rev., 26, 223–257, 2007.

DeCarlo, P. F., Kimmel, J. R., Trimborn, A., Northway, M. J., Jayne, J. T., Aiken, A. C., Gonin, M., Fuhrer, K., Horvath, T., and Docherty, K. S.: Field-deployable, high-resolution, time-of-flight aerosol mass spectrometer, Anal. Chem., 78, 8281–8289, 2006.

Ehn, M., Junninen, H., Petaj a, T., Kurtén, T., Kerminen, V.-M., Schobesberger, S., Manninen, H. E., Ortega, I. K., Vehkamäki, H., Kulmala, M., and Worsnop, D. R.: Composition and temporal behavior of ambient ions in the boreal forest, Atmos. Chem. Phys., 10, 8513–8530, 2010.

Ehn, M., Thornton, J. A., Kleist, E., Sipila, M., Junninen, H., Pullinen, I., Springer, M., Rubach, F., Tillmann, R., Lee, B., LopezHilfiker, F., Andres, S., Acir, I.-H., Rissanen, M., Jokinen, T., Schobesberger, S., Kangasluoma, J., Kontkanen, J., Nieminen, T., Kurtén, T., Nielsen, L. B., Jørgensen, S., Kjaergaard, H. G., Canagaratna, M., Maso, M. D., Berndt, T., Petaja, T., Wahner, A., Kerminen, V.-M., Kulmala, M., Worsnop, D. R., Wildt, J., and Mentel, T. F.: A large source of low-volatility secondary organic aerosol, Nature, 506, 476–479, 2014.

Foley, K. M., Roselle, S. J., Appel, K. W., Bhave, P. V., Pleim, J. E., Otte, T. L., Mathur, R., Sarwar, G., Young, J. O., Gilliam, R. C., Nolte, C. G., Kelly, J. T., Gilliland, A. B., and Bash, J. O.: Interactive comment on “Incremental testing of the community multiscale air quality (CMAQ) modeling system version 4.7”, Geosci. Model Dev. Discuss., 2, C515–C532, 2010.

Gao, S., Surratt, J. D., Knipping, E. M., Edgerton, E. S., Shahgholi, M., and Seinfeld, J. H.: Characterization of polar organic components in fine aerosols in the southeastern United States: Identity, origin, and evolution, J. Geophys. Res. Atmos., 111, D07302, 2006.

Gómez-González, Y., Surratt, J. D., Cuyckens, F., Szmigielski, R., Vermeylen, R., Jaoui, M., Lewandowski, M., Offenberg, J. H., Kleindienst, T. E., Edney, E. O., Blockhuys, F., Van Alsenoy, C., Maenhaut, W., and Claeys, M.: Characterization of organosulfates from the photooxidation of isoprene and unsaturated fatty acids in ambient aerosol using liquid chromatography/(-) electrospray ionization mass spectrometry, J. Mass Spectrom., 43, 371–382, 2008.

Guo, S., Hu, M., Wang, Z. B., Slanina, J., and Zhao, Y. L.: Size-resolved aerosol water-soluble ionic compositions in the summer of Beijing: implication of regional secondary formation, Atmos. Chem. Phys.,10, 947-959, 2010.

Guo, S., Hu, M, Guo, Q. F., Zhang, X., Zheng, M., Zheng, J., Chang, C. C., Schauer, J. J., and Zhang, R. Y.: Primary sources and secondary formation of organic aerosols in Beijing, China, Environ. Sci. Technol., 46, 18, 9846-9853, 2012.

Guo, S., Hu, M., Guo, Q. F., Zhang, X., Schauer, J. J., and Zhang R. Y.: Quantitative evaluation of emission control of primary and secondary organic aerosol sources during Beijing 2008 Olympics, Atmos. Chem. Phys., 13, 8303–8314, 2013.

Guo, S., Hu, M., Zamora, M, Peng, J. F., Shang, D. J., Zheng, J., Du Z. F., Wu, Z. J., Shao, M., Zeng, L. M., Molina, M., and Zhang, R.: Elucidating severe urban haze formation in China, PNAS, 111, 49, 17373-17378, 2014.

Hallquist, M., Wenger, J. C., Baltensperger, U., Rudich, Y., Simpson, D., Claeys, M., Dommen, J., Donahue, N. M., George, C., Goldstein, A. H., Hamilton, J. F., Herrmann, H., Hoffmann, T., Iinuma, Y., Jang, M., Jenkin, M. E., Jimenez, J. L., Kiendler-Scharr, A., Maenhaut, W., McFiggans, G., Mentel, Th. F., Monod, A., Prévôt, A. S. H., Seinfeld, J. H., Surratt, J. D., Szmigielski, R., and Wildt, J.: The formation, properties and impact of secondary organic aerosol: current and emerging issues, Atmos. Chem. Phys., 9, 5155–5236, doi:10.5194/acp-9-5155- 2009, 2009.

Hallquist, M., Munthe, J., Hu, M., Mellqvist, J., Wang, T., Chan, C. K., Gao, J., Boman, J., Guo, S., Hallquist, Å. M., Moldanova, J., Pathak, R. K., Pettersson, J. B. C., Pleijel, H., Simpson, D., and Thynell, M.: Photochemical smog in china: Scientific challenges and implications for air quality policies, Nat. Sci. Rev., 3, 401-403, 2016.

Hansen, A. M. K., Kristensen, K., Nguyen, Q. T., Zare, A., Cozzi, F., Nøjgaard, J. K., Skov, H., Brandt, J., Christensen, J. H., Ström, J., Tunved, P., Krejci, R., and Glasius, M.: Organosulfates and organic acids in Arctic aerosols: speciation, annual variation and concentration levels, Atmos. Chem. Phys., 14, 7807–7823, 2014.

Hansen, A. M. K., Hong, J., Raatikainen, T., Kristensen, K., Ylisirniö, A., Virtanen, A., Petäjä, T., Glasius, M., and Prisle, N. L.: Hygroscopic properties and cloud condensation nuclei activation of limonene-derived organosulfates and their mixtures with ammonium, Atmos. Chem. and Phys., 15, 14071-14089, 2015.

Harrison, M. A. J., Barra, S., Borghesi, D., Vione, D., Arsene, C., and Iulian Olariu, R.: Nitrated phenols in the atmosphere: a review, Atmos. Environ., 39, 231–248, 2005.

Heald, C. L., Jacob, D. J., Park, R. J., Russell, L. M., Huebert, B. J., Seinfeld, J. H., Liao, H., and Weber, R. J.: A large organic aerosol source in the free troposphere missing from current models, Geophys. Res. Lett., 32, L18809, 2005.

Hettiyadura, A. P. S., Stone, E. A., Kundu, S., Baker, Z., Geddes, E., Richards, K., and Humphry, T.: Determination of atmospheric organosulfates using HILIC chromatography with MS detection, Atmos. Meas. Tech., 8, 2347–2358, 2015.

Hettiyadura, A. P. S., Jayarathne, T., Baumann, K., Goldstein, A. H., de Gouw, J. A., Koss, A., Keutsch, F. N., Skog, K., and Stone, E. A.: Qualitative and quantitative analysis of atmospheric organosulfates in Centreville, Alabama, Atmos. Chem. Phys., 17, 1343-1359, 2017.

Hilpert, K.: Potential of mass spectrometry for the analysis of inorganic high temperature vapors, Fresen. J. Anal. Chem., 370, 471–478, 2001.

Hu, W., Hu, M., Jiminez, J. L., Tang, Q., Peng, J. F., Hu, W., Shao, M., Wang, M., Zeng, L. M., Wu, Y. S., Gong, Z. H., Huang, X. F., and He, K. Y.: Insights on organic aerosol aging and the influence of coal combustion at a regional receptor site of central eastern China, Atmos. Chem. Phys., 13, 10095-10112, 2013.

Hu, W., Hu, M., Hu, W., Jimenez, J. L., Yuan, B., Chen, W., Wang, M., Wu, Y., Chen, C., Wang, Z., Peng, J., Yang, K., Zeng, L., and Shao, M.: Chemical composition, sources and aging process of sub-micron aerosols in Beijing: contrast between summer and winter, J. Geophys. Res. Atmos., 121, 1955–1977, 2016.

Hu, W., Hu, M., Hu, W. W., Zheng, J., Chen, C., Wu, Y., and Guo, S.: Seasonal variations of high time-resolved chemical compositions, sources and evolution for atmospheric submicron aersols in the megacity Beijing, Atmos. Chem. Phys. Discuss., 2017, 1-43, 2017.

Huang, D. D., Li, Y. J., Lee, B. P., and Chan, C. K.: Analysis of Organic Sulfur Compounds in Atmospheric Aerosols at the HKUST Supersite in Hong Kong Using HR-ToF-AMS, Environ. Sci. Technol., 49, 3672–3679, 2015.

Huang, X. F., He, L. Y., Hu, M., Canagaratna, M. R., Sun, Y., Zhang, Q., Zhu, T., Xue, L., Zeng, L. W., Liu, X. G., Zhang, Y. H., Jayne, J. T., Ng, N. L., and Worsnop, D. R.: Highly time-resolved chemical characterization of atmospheric submicron particles during 2008 Beijing olympic games using an Aerodyne high-Resolution aerosol mass spectrometer, Atmos. Chem. Phys., 10(18), 8933-8945, 2010.

Iinuma, Y., Muller, C., Berndt, T., Boge, O., Claeys, M., and Herrmann, H.: Evidence for the existence of organosulfates from beta-pinene ozonolysis in ambient secondary organic aerosol, Environ. Sci. Technol., 41, 19, 6678-6683, 2007.

Inomata, S., Tanimoto, H., Fujitani, Y., Sekimoto, K., Sato, K., Fushimi, A., Yamada, H., Hori, S., Kumazawa, Y., Shimono, A., and Hikida, T.: On-line measurements of gaseous nitro-organic compounds in diesel vehicle exhaust by proton-transfer-reaction mass spectrometry, Atmos. Environ., 73, 195–203, 2013.

Jokinen, T., Sipilä, M., Richters, S., Kerminen, V.-M., Paasonen, P., Stratmann, F., Worsnop, D., Kulmala, M., Ehn, M., Herrmann, H., and Berndt, T.: Rapid autoxidation forms highly oxidized RO2 radicals in the atmosphere, Angew. Chem. Int. Edit., 53, 14596–14600, doi:10.1002/anie.201408566, 2014.

Kim, J. Y., Lee, E. Y., Choi, I., Kim, J., and Cho, K. H.: Effects of the particulate matter2.5 (PM1) on lipoprotein metabolism, uptake and degradation, and embryo toxicity, Mol Cells., 38, 12, 1096-1104, 2015.

Krieger, U. K., Siegrist, F., Marcolli, C., Emanuelsson, E. U., Gøbel, F. M., Bilde, M., Marsh, A., Reid, J. P., Huisman, A. J., Riipinen, I., Hyttinen, N., Myllys, N., Kurtén, T., Bannan, T., and Topping, D.: A reference data set for validating vapor pressure measurement techniques: Homologous series of polyethylene glycols, Atmos. Meas. Tech. Discuss., https://doi.org/10.5194/amt-2017-224, in review, 2017.

Kristensen, K. and Glasius, M.: Organosulfates and oxidation products from biogenic hydrocarbons in fine aerosols from a forest in North West Europe during spring, Atmos. Environ., 45, 4546–4556, 2011.

Kristensen, K., Bilde, M., Aalto, P. P., Petäjä, T., and Glasius, M.: Denuder/filter sampling of organic acids and organosulfates at urban and boreal forest sites: gas/particle distribution and possible sampling artifacts. Atmos. Environ., 130, 36-53, 2016.

Lee, B. H., Mohr, C., Lopez-Hilfiker, F. D., Lutz, A., Hallquist, M., Lee, L., Romer, P., Cohen, R. C., Iyer, S., Kurtén, T., Hu, W., Day, D. A., Campuzano-Jost, P., Jimenez, J. L., Xu, L., Ng, N. L., Guo, H., Weber, R. J., Wild, R. J., Brown, S. S., Koss, A., de Gouw, J., Olson, K., Goldstein, A. H., Seco, R., Kim, S., McAvey, K., Shepson, P. B., Starn, T., Baumann, K., Edgerton, E. S., Liu, J., Shilling, J. E., Miller, D. O., Brune, W., Schobesberger, S., D'Ambro, E. L., and Thornton, J. A.: Highly functionalized organic nitrates in the southeast United States: Contribution to secondary organic aerosol and reactive nitrogen budgets, P. Natl. Acad. Sci. USA, 113, 1516–1521 doi:10.1073/pnas.1508108113, 2016.

Le Breton, M., McGillen, M. R., Muller, J. B. A., Bacak, A., Shallcross, D. E., Xiao, P., Huey, L. G., Tanner, D., Coe, H., and Percival, C. J.: Airborne observations of formic acid using a chemical ionization mass spectrometer, Atmos. Meas. Tech., 5, 3029–3039, 2012.

Le Breton, M., Bacak, A., Muller, J. B. A., O'Shea, S. J., Xiao, P., Ashfold, M. N. R., Cooke, M. C., Batt, R., Shallcross, D. E., Oram, D. E., Forster, G., Bauguitte, S. J.-B., Palmer, P. I., Parrington, M., Lewis, A. C., Lee, J. D., and Percival, C. J.: Airborne hydrogen cyanide measurements using a chemical ionisation mass spectrometer for the plume identification of biomass burning forest fires, Atmos. Chem. Phys., 13, 9217– 9232, 2013.

Le Breton, M., Bacak, A., Muller, J. B. A., Bannan, T. J., Kennedy, O., Ouyang, B., Xiao, P., Bauguitte, S. J. B., Shallcross, D. E., Jones, R. L., Daniels, M. J. S., Ball, S. M., and Percival, C. J.: The first airborne comparison of N2O5 measurements over the UK using a CIMS and BBCEAS during the RONOCO campaign, Anal. Methods-UK, 6, 9731-9743, 2014.

Li, Y. J., Sun, Y., Zhang, Q., Li, X., Li, M., Zhou, Z., and Chan, C.: Real-time chemical characterization of atmospheric particulate matter in China: A review, Atmos. Environ., 158, 270-304, 2017.

Liao, J., Froyd, K. D., Murphy, D. M., Keutsch, F. N., Yu, G., Wennberg, P. O., St. Clair, J. M., Crounse, J. D., Wisthaler, A., Mikoviny, T., Jimenez, J. L., Campuzano-Jost, P., Day, D. A., Hu, W., Ryerson, T. B., Pollack, I. B., Peischl, J., Anderson, B. E., Ziemba, L. D., Blake, D. R., Meinardi, S., and Diskin, G.: Airborne measurements of organosulfates over the continental U.S, J. Geophys. Res. Atmos., 120, 2990–3005, 2015.

Lin, P., Yu, J. Z., Engling, G., and Kalberer, M.: Organosulfates in humic-like substance fraction isolated from aerosols at seven locations in East Asia: A study by ultra-high-Resolution mass spectrometry, Environ. Sci. Technol., 46, 13118–13127, 2012.

Lopez-Hilfiker, F. D., Mohr, C., Ehn, M., Rubach, F., Kleist, E., Wildt, J., Mentel, Th. F., Lutz, A., Hallquist, M., Worsnop, D., and Thornton, J. A.: A novel method for online analysis of gas and particle composition: description and evaluation of a Filter Inlet for Gases and AEROsols (FIGAERO), Atmos. Meas. Tech., 7, 983–1001, 2014.

Mohr, C., Lopez-Hilfiker, F. D., Zotter, P., Prévôt, A. S. H., Xu, L., Ng, N. L., Herndon, S. C., Williams, L. R., Franklin, J. P., Zahniser, M. S., Worsnop, D. R., Knighton, W. B., Aiken, A. C., Gorkowski, K. J., Dubey, M. K., Allan, J. D., and Thornton, J. A.: Contribution of nitrated phenols to wood burning brown carbon light absorption in Detling, United Kingdom during winter time, Environ. Sci. Technol., 47, 6316–6324, 2013.

Murphy, D. M., Cziczo, D. J., Hudson, P. K., and Thomson, D. S.: Carbonaceous material in aerosol particles in the lower stratosphere and tropopause region, J. Geophys. Res., 112, 2007.

Nozière, B., Ekstrom, S., Alsberg, T., and Holmstrom, S.: Radical-initiated formation of organosulfates and surfactants in atmospheric aerosols, Geophys. Res. Lett., 37, 2010.

Olson, C. N., Galloway, M. M., Yu, G., Hedman, C. J., Lockett, M. R., Yoon, T., Stone, E. A., Smith, L. M., and Keutsch, F. N.: Hydroxycarboxylic acid-derived organosulfates: Synthesis, stability, and quantification in ambient aerosol, Environ. Sci. Technol., 45, 15, 6468–6474, 2011.

Pope, C. A., Burnett, R. T., Thun, M. J., Calle, E. E., Krewski, D., Ito, K., and Thurston, G. D.: Lung cancer, cardiopulmonary mortality, and long-term exposure to fine particulate air pollution, J. Am. Med. Assoc., 287(9), 1132–1141, 2002.

Reemtsma, T., Weiss, S., Mueller, J., Petrovic, M., Gonzalez, S., Barcelo, D., Ventura, F., and Knepper, T. P.: Polar pollutants entry into the water cycle by municipal wastewater: A European perspective, Environ. Sci. Tech. 40, 2006.

Riva, M., Tomaz, S., Cui, T., Lin, Y-H, Perraudin, E., Gold, A., Stone, E. A., Villenave, E., and Surratt, J. D.: Evidence for an unrecognized secondary anthropogenic source of organosulfates and sulfonates: gas-phase oxidation of polycyclic aromatic hydrocarbons in the presence of sulfate aerosol, Environ. Sci. Technol., 49 (11), 6654–6664, 2015.

Riva, M., Da Silva Barbosa, T., Lin, Y.-H., Stone, E. A., Gold, A., and Surratt, J. D.: Chemical characterization of organosulfates in secondary organic aerosol derived from the photooxidation of alkanes, Atmos. Chem. Phys., 16, 11001-11018, https://doi.org/10.5194/acp-16-11001-2016, 2016.

Schindelka, J., Iinuma, Y., Hoffmann, D., and Herrmann, H.: Sulfate radical-initiated formation of isoprene-derived organosulfates in atmospheric aerosols, Faraday Discuss., 165,237–259, 2013.

Shalamzari, M. S., Ryabtsova, O., Kahnt, A., Vermeylen, R., Herent, M. F., Quetin-Leclercq, J., Van der Veken, P., Maenhaut, W., and Claeys, M.: Mass spectrometric characterization of organosulfates related to secondary organic aerosol from isoprene, Rapid Commun. Mass Spectrom., 784–794, 2013.

Shalamzari, S. M., Ryabtsova, O., Kahnt, A., Vermeylen, R., Hérent, M.-F., Quetin-Leclercq, J., Van Der Veken, P., Maenhaut, W., and Claeys, M.: Mass spectrometric characterization of organosulfates related to secondary organic aerosol from isoprene, Rapid Commun. Mass Spectrom., 27, 784–794, 2013. Shalamzari, M. S., Kahnt, A., Vermeylen, R., Kleindienst, T. E., Lewandowski, M., Cuyckens, F., Maenhaut, W., and Claeys, M.: Characterization of polar organosulfates in secondary organic aerosol from the green leaf volatile 3-Z-hexenal, Environ. Sci. Technol., 48, 12671–12678, 2014.

Smith, J. N., Dunn, M. J., VanReken, T. M., Iida, K., Stolzenburg, M. R, McMurry, P. H., and Huey, L. G.: Chemical composition of atmospheric nanoparticles formed from nucleation in Tecamac, Mexico: Evidence for an important role for organic species in nanoparticle growth, Geophys. Res. Lett., 35, 4, 2008.

Stark, H., R. L. N. Yatavelli, S. L. Thompson, H. Kang, J. E. Krechmer, J. R. Kimmel, B. B. Palm, W. Hu, P. L. Hayes, D. A. Day, P. Campuzano-Jost, M. R. Canagaratna, J. T. Jayne, D. R. Worsnop, and J. L. Jimenez: Impact of Thermal Decomposition on Thermal Desorption Instruments: Advantage of Thermogram Analysis for Quantifying Volatility Distributions of Organic Species, Environ Sci Technol, doi:10.1021/acs.est.7b00160, 2017.

Staudt, S., Kundu, S., He, X., Lehmler, H. J., Lin, Y. H., Cui, T. Q., Kristensen, K., Glasius, M., Zhang, X., Weber, R., Surratt, J. D., and Stone, E. A.: Aromatic organosulfates in atmospheric aerosols: Synthesis, characterization, and abundance, Atmos. Environ., 94, 366–373, 2014.

Stone, E. A., Yang, L., Yu, L. E., and Rupakheti, M.: Characterization of organosulfates in atmospheric aerosols at Four Asian locations, Atmos. Environ., 47, 323–329, 2012.

Surratt, J. D., Lewandowski, M., Offenberg, J. H., Jaoui, M., Kleindienst, T. E., Edney, E. O., and Seinfeld, J. H.: Effect of acidity on secondary organic aerosol formation from isoprene, Environ. Sci. Technol., 41, 5363–5369, 2017.

Surratt, J. D., Gomez-Gonzalez, Y., Chan, A. W. H., Vermeylen, R., Shahgholi, M., Kleindienst, T. E., Edney, E. O., Offenberg, J. H., Lewandowski, M., Jaoui, M., Maenhaut, W., Claeys, M., Flagan, R. C., and Seinfeld, J. H.: Organic sulfate formation in biogenic secondary organic aerosol, J. Phys. Chem., 112, 8345– 8378, 2008.

Surratt, J. D., Chan, A. W. H., Eddingsaas, N. C., Chan, M. N., Loza, C. L., Kwan, A. J., Hersey, S. P., Flagan, R. C., Wennberg, P. O., and Seinfeld, J. H.: Reactive intermediates revealed in secondary organic aerosol formation from isoprene, Proc. Natl. Acad. Sci. U.S.A. 2010.

Wang, X. K., Rossignol, S., Ma, Y., Yao, L., Wang, M., Chen, J. M., George, C. and Wang, L.: Molecular characterization of atmospheric particulate organosulfates in three megacities at the middle and lower reaches of the Yangtze River, Atmos. Chem. Phys., 16, 2285-2298, 2016.

Worton, D. R., Surratt, J. D., Lafranchi, B. W., Chan, A. W., Zhao, Y., Weber, R. J., Park, J. H., Gilman, J. B., de Gouw, J., Park, C., Schade, G., Beaver, M., Clair, J. M., Crounse, J., Wennberg, P., Wolfe, G. M., Harrold, S., Thornton, J. A., Farmer, D. K., Docherty, K. S., Cubison, M. J., Jimenez, J. L., Frossard, A. A., Russell, L. M., Kristensen, K., Glasius, M., Mao, J., Ren, X., Brune, W., Browne, E. C., Pusede, S. E., Cohen, R. C., Seinfeld, J. H., and Goldstein, A. H.: Observational insights into aerosol formation from isoprene, Environ. Sci. Technol., 47, 11403–11413, 2013.

Wuebbles, D. J. and Jain, A. K.: Concerns about climate change and the role of fossil fuel use, Fuel. Process. Techn., 71, 99-119, 2001.

Zhang, H., Worton, D. R., Lewandowski, M., Ortega, J., Rubitschun, C. L., Park, J.-H., Kristensen, K., Campuzano-Jost, P., Day, D. A., Jimenez, J. L., Jaoui, M., Offenberg, J. H., Kleindienst, T. E., Gilman, J., Kuster, W. C., de Gouw, J., Park, C., Schade, G. W., Frossard, A. A., Russell, L., Kaser, L., Jud, W., Hansel, A., Cappellin, L., Karl, T., Glasius, M., Guenther, A., Goldstein, A. H., Seinfeld, J. H., Gold, A., Kamens, R. M., and Surratt, J. D.: Organosulfates as tracers for secondary organic aerosol (SOA) formation from 2-methyl-3-buten-2-ol (MBO) in the atmosphere, Environ. Sci. Technol., 46, 9437–9446, 2012b.

Zhang, Q., He, K., and Huo, H.: Policy: Cleaning China’s air, Nature, 484, 161–162, 2012a.

Zhang, Q., Jimenez, J. L., Worsnop, D. R., and Canagaratna, M.: A case study of urban particle acidity and its influence on secondary organic aerosol, Environ. Sci. Technol. 2007.

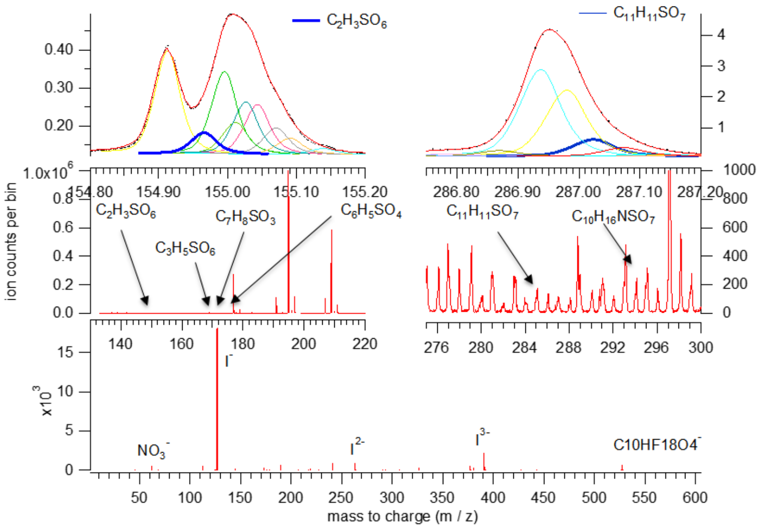

$C_2H_3SO_6$
$C_{11}H_{11}SO_7$
0.40
0.30
0.20
4
3
2
1
154.80
154.90
155.00
155.10
155.20
286.80
286.90
287.00
287.10
287.20
1.0x10^6
0.8
0.6
0.4
0.2
0.0
1000
800
600
400
200
0
ion counts per bin
$C_2H_3SO_6$
$C_3H_5SO_6$
$C_7H_8SO_3$
$C_6H_5SO_4$
$C_{11}H_{11}SO_7$
$C_{10}H_{16}NSO_7$
140
160
180
200
220
276
280
284
288
292
296
300
x10^3
15
10
5
0
I^-
NO_3^-
I^{2-}
I^{3-}
C10HF18O4$^-$
50
100
150
200
250
300
350
400
450
500
550
600
mass to charge (m / z)

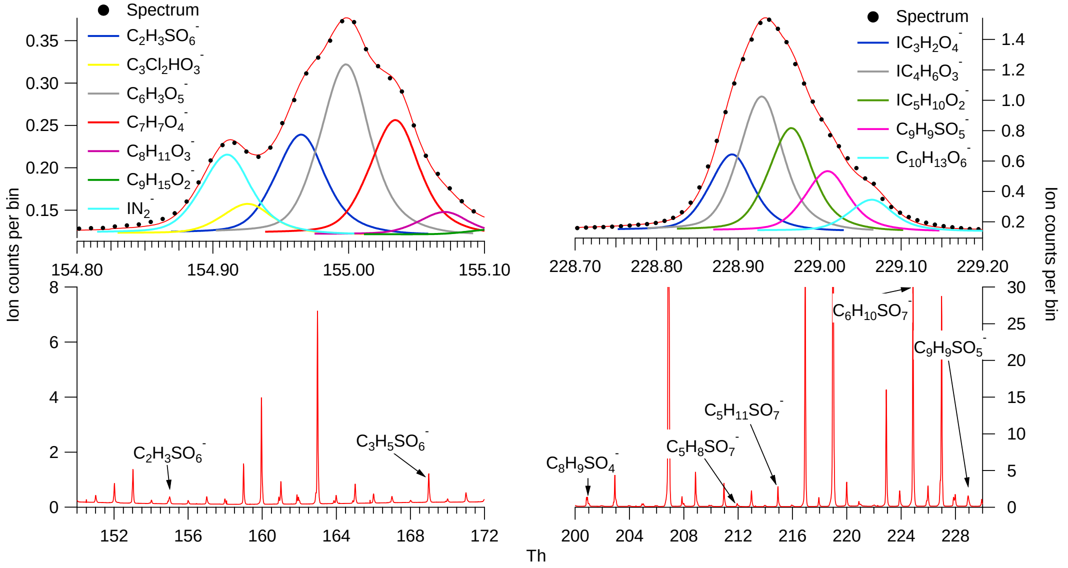

Spectrum
$C_2H_3SO_6^-$
$C_3Cl_2HO_3^-$
$C_6H_3O_5^-$
$C_7H_7O_4^-$
$C_8H_{11}O_3^-$
$C_9H_{15}O_2^-$
IN_2^-
0.35
0.30
0.25
0.20
0.15
154.80
154.90
155.00
155.10
Spectrum
$IC_3H_2O_4^-$
$IC_4H_6O_3^-$
$IC_5H_{10}O_2^-$
$C_9H_9SO_5^-$
$C_{10}H_{13}O_6^-$
1.4
1.2
1.0
0.8
0.6
0.4
0.2
228.70
228.80
228.90
229.00
229.10
229.20
Ion counts per bin
8
6
4
2
0
$C_2H_3SO_6^-$
$C_3H_5SO_6^-$
152
156
160
164
168
172
$C_8H_9SO_4^-$
$C_5H_8SO_7^-$
$C_5H_{11}SO_7^-$
$C_6H_{10}SO_7^-$
$C_9H_9SO_5^-$
30
25
20
15
10
5
0
200
204
208
212
216
220
224
228
Th
Ion counts per bin

Figure 1. The bottom panel displays the average campaign mass ~~spectra~~spectrum for the whole mass range of the ToF (3-620) which is further expanded to show small regions in the middle panel and specific and HR fitting for individual peaks in the top panel.

Table 1. SCOs identified at the Changping site with their respective mass, chemical name and potential precursors.

m/z ion	Molecular formula	Reference	OS name	Precursor	[mean] µgm-3	mean % PM	% OS
217.9759	$C_6H_4NSO_6^-$	-	Nitrophenol sulphate	Nitrophenol	2.60	0.00	0.4
154.965582	$C_2H_3SO_6^-$	Surrat 2007	Glycolic acid sulphate	Glycolic acid	9.60	0.03	1.6
168.981232	$C_3H_5SO_6^-$	Olson 2011	Lactic acid sulphate	Lactic acid	35.00	0.12	5.9
171.012139	$C_7H_7SO_3^-$	Riva 2015		Aromatics (Benzene and PAHs)	16.00	0.06	2.7
172.019964	$C_7H_8SO_3^-$	Riva 2015		Aromatics (Benzene and PAHs)	5.40	0.02	0.9
184.991403	$C_7H_5SO_4^-$	Riva 2015		Aromatics (Benzene and PAHs)	72.00	0.25	12.1
187.007053	$C_7H_7SO_4^-$	Staudt 2014	Methyl phenyl sulphate	benzene	40.00	0.14	6.7
199.007053	$C_8H_7SO_4^-$	Riva 2015		Aromatics (Benzene and PAHs)	14.00	0.05	2.4
199.999622	$C_4H_8SO_7^-$	Surrat 2007		2-methylglyceric acid (isoprene)	5.00	0.02	0.8
201.022703	$C_8H_9SO_4^-$	Staudt 2014	4 methyl benzyl sulphate	benzene	22.00	0.08	3.7
211.999622	$C_5H_8SO_7^-$	Surrat 2008		isoprene	8.00	0.03	1.3
215.023097	$C_5H_{11}SO_7^-$	Surrat 2010	IEPOX sulphate	IEPOX	27.00	0.09	4.5
226.015272	$C_6H_{10}SO_7^-$	Boris 2016	unknown	unknown	90.00	0.31	15.1
229.017618	$C_9H_9SO_5^-$	Riva 2015		Aromatics (Benzene and PAHs)	30.00	0.10	5.0
231.033268	$C_9H_{11}SO_5^-$	Riva 2015		Aromatics (Benzene and PAHs)	40.00	0.14	6.7
287.023097	$C_{11}H_{11}SO_7^-$	Riva 2015		Aromatics (Benzene and PAHs)	120.00	0.41	20.2
294.065296	$C_{10}H_{16}NSO_7^-$	Surrat 2008		alpha pinene	58.80	0.20	9.9

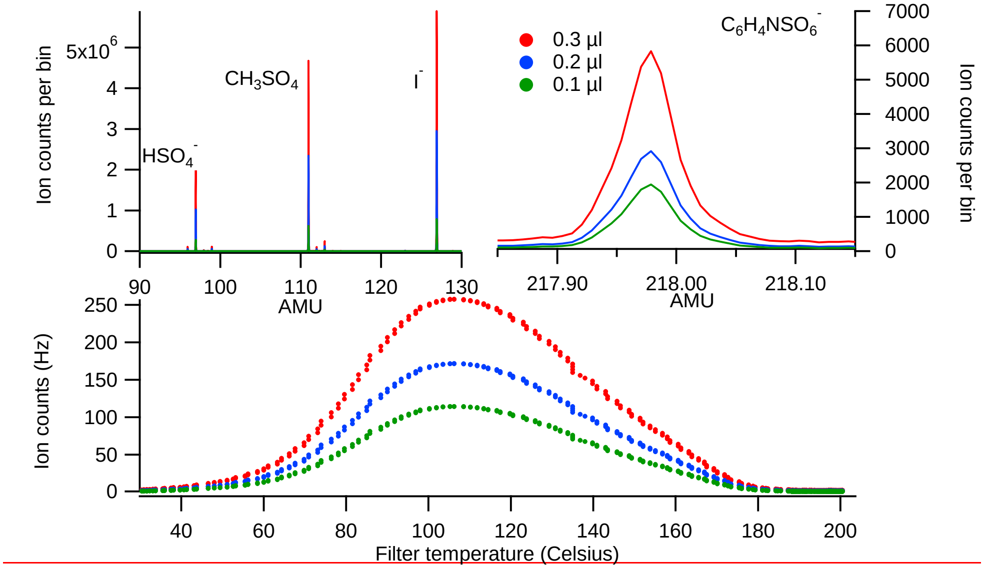

m/z ion	Molecular formula	Reference	OS name	Precursor	[mean] µgm-3	mean % PM	mean % OA	mean % OS
154.965582	$C_2H_3SO_6^-$	Surrat 2007	Glycolic acid sulphate	Glycolic acid	2.97	0.02	0.03	1.6
168.981232	$C_3H_5SO_6^-$	Olson 2011	Lactic acid sulphate	Lactic acid	13.00	0.07	0.14	5.9
171.012139	$C_7H_7SO_3^-$	Riva 2015		Aromatics (Benzene and PAHs)	6.00	0.03	0.06	2.7
172.019964	$C_7H_8SO_3^-$	Riva 2015		Aromatics (Benzene and PAHs)	4.00	0.02	0.04	0.9
184.991403	$C_7H_5SO_4^-$	Riva 2015		Aromatics (Benzene and PAHs)	24.00	0.12	0.25	12.1
187.007053	$C_7H_7SO_4^-$	Staudt 2014	Methyl phenyl sulphate	benzene	14.00	0.07	0.15	6.7
199.007053	$C_8H_7SO_4^-$	Riva 2015		Aromatics (Benzene and PAHs)	5.00	0.03	0.05	2.4
199.999622	$C_4H_8SO_7^-$	Surrat 2007		2-methylglyceric acid (isoprene)	3.00	0.02	0.03	0.8
201.022703	$C_8H_9SO_4^-$	Staudt 2014	4 methyl benzyl sulphate	benzene	6.00	0.03	0.06	3.7
211.999622	$C_5H_8SO_7^-$	Surrat 2008		isoprene	2.00	0.01	0.02	1.3
215.023097	$C_5H_{11}SO_7^-$	Surrat 2010	IEPOX sulphate	IEPOX	11.00	0.06	0.12	4.5
217.9759	$C_6H_4NSO_6^-$	-	Nitrophenol sulphate	Nitrophenol	1.00	0.01	0.01	0.4
226.015272	$C_6H_{10}SO_7^-$	Boris 2016	unknown	unknown	30.00	0.16	0.32	15.1
229.017618	$C_9H_9SO_5^-$	Riva 2015		Aromatics (Benzene and PAHs)	10.00	0.05	0.11	5.0
231.033268	$C_9H_{11}SO_5^-$	Riva 2015		Aromatics (Benzene and PAHs)	13.00	0.07	0.14	6.7
287.023097	$C_{11}H_{11}SO_7^-$	Riva 2015		Aromatics (Benzene and PAHs)	40.00	0.21	0.42	20.2
294.065296	$C_{10}H_{16}NSO_7^-$	Surrat 2008		alpha pinene	21.00	0.00	0.22	9.9

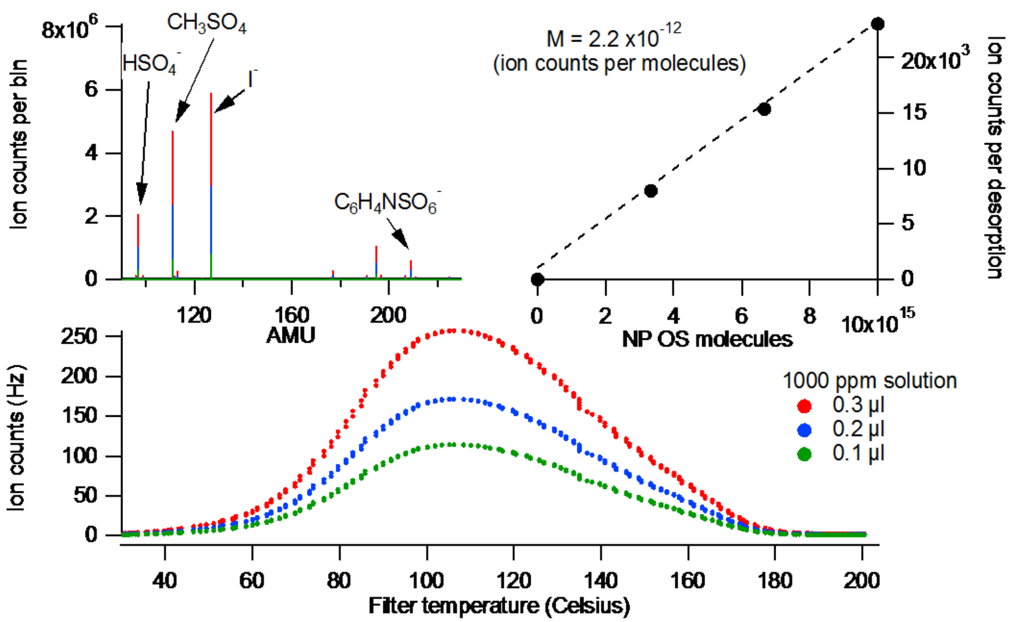

Figure 2. The ~~time series~~desorption profile of ~~the~~ NP OS 3 step ~~calibration time series~~calibrations for 0.1 µl, 0.2 µl and 0.3 µl 1000 ppm solution is displayed in the bottom panel and its corresponding average stick spectra (top left) and ~~HR~~sum of counts per molecule loading for each calibration (top right) ~~intensities and peak shapes for the desorption.~~

~~Table 2. The mean campaign mass, percentage contribution to PM$_1$ and percent contribution to total SCOs for each SCO identified in this work.~~

Formatted: Font: Not Bold, Font color: Auto, Pattern: Clear

Formatted: Centered

Molecular formula	[mean] ngm-3	mean % OA	% SCO	Molecular formula	[mean] ngm-3	mean % OA	% SCO
C11H11SO7-	40	0.40	19.45	**C8H9SO4-**	6	0.06	3.05
C6H10SO7-	30	0.30	14.63	**C7H7SO3-**	6	0.06	2.89
C7H5SO4-	24	0.23	11.41	**C8H7SO4-**	5	0.05	2.25
C10H16NSO7-	21	0.20	9.97	**C7H8SO3-**	4	0.04	2.09
C7H7SO4-	14	0.14	6.75	**C2H3SO6-**	4	0.04	1.93
C9H11SO5-	13	0.13	6.27	**C4H8SO7-**	3	0.03	1.45
C3H5SO6-	13	0.12	6.11	**C5H8SO7-**	2	0.02	1.13
C5H11SO7-	11	0.11	5.47	**C6H4NSO6-**	1	0.01	0.48
C9H9SO5-	10	0.09	4.66	**Sum SCO**	207	2	100

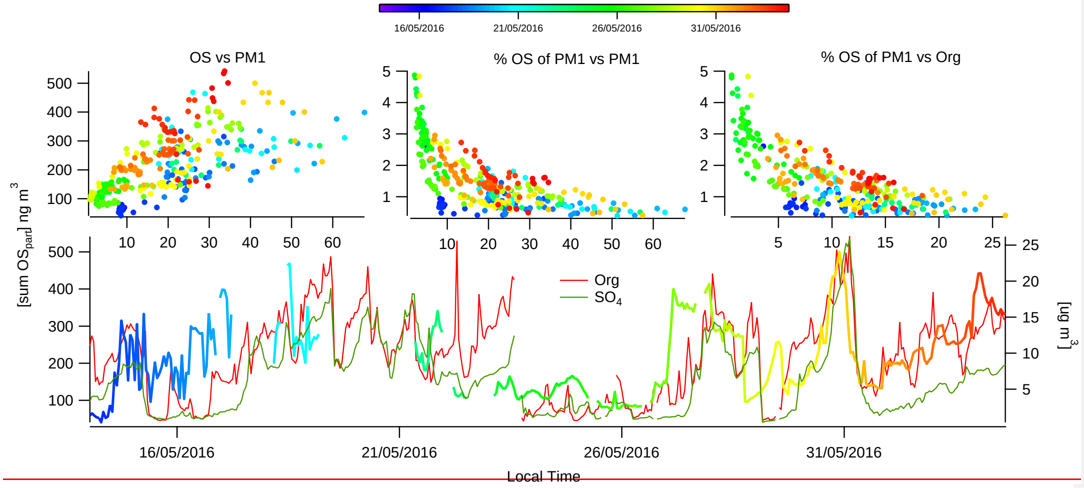

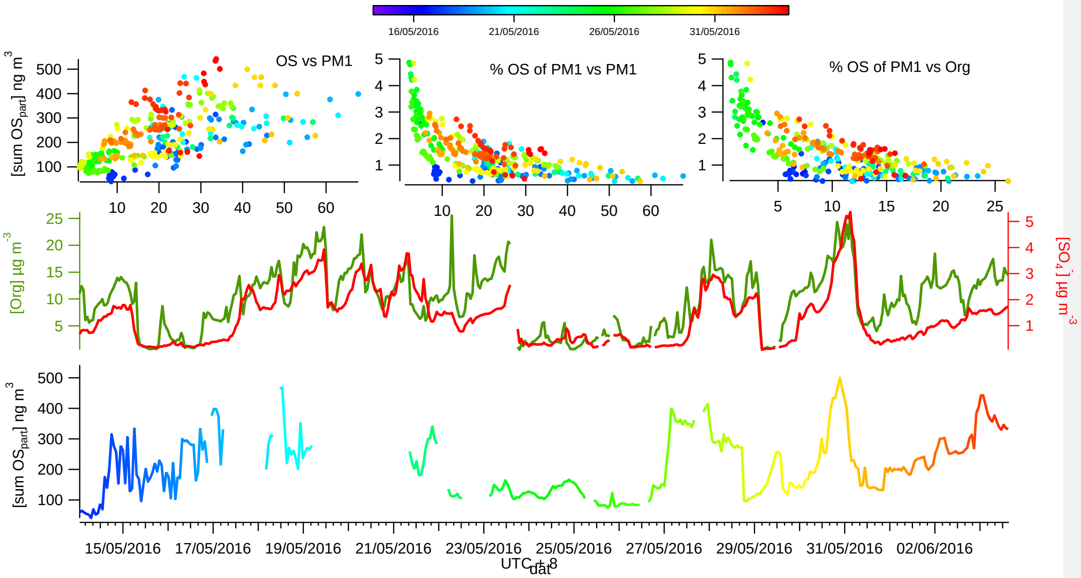

Figure 3. Time series of ~~organics (green), SO_4^{2-} (red) and~~ total SCO (colour coded with time) is displayed in the bottom panel. ~~The~~The time series of the AMS organic (green) and sulfate (red) is displayed in the middle panel and the correlation of SCO to PM_1, mass fraction of PM_1 and organics are displayed in the upper panel. The colour coding represents time throughout the campaign.

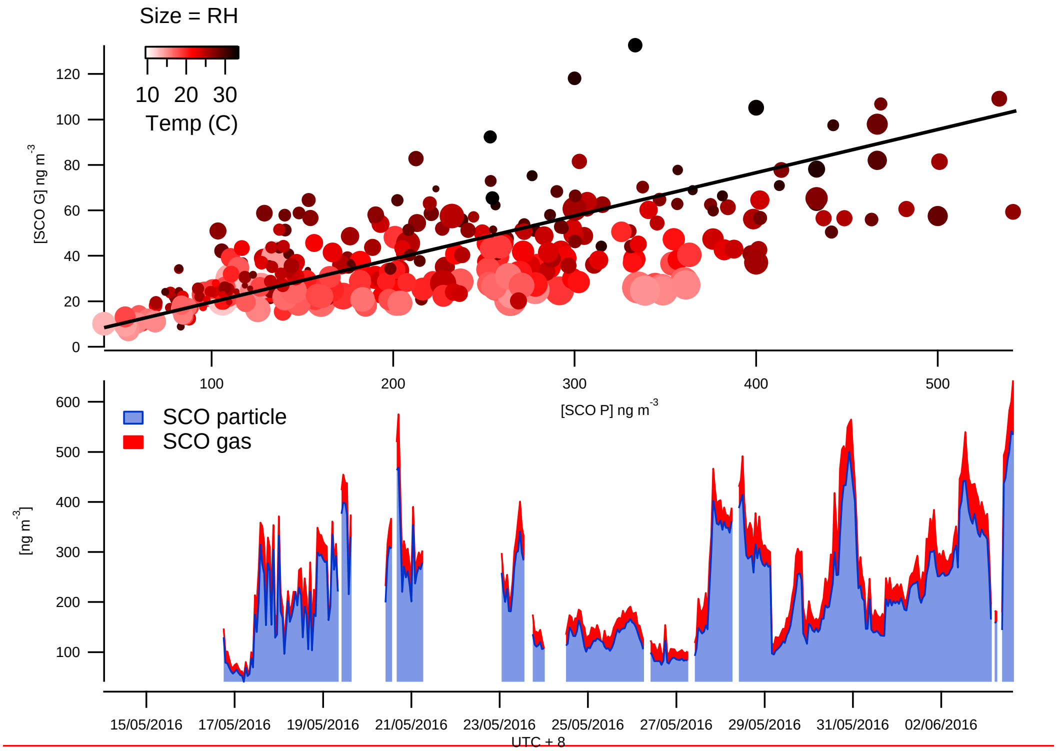

Size = RH
10 20 30
Temp (C)
[SCO G] ng m-3
0
20
40
60
80
100
120
100
200
300
400
500
[SCO P] ng m-3
SCO particle
SCO gas
[ng m-3]
100
200
300
400
500
600
15/05/2016
17/05/2016
19/05/2016
21/05/2016
23/05/2016
25/05/2016
27/05/2016
29/05/2016
31/05/2016
02/06/2016
UTC + 8

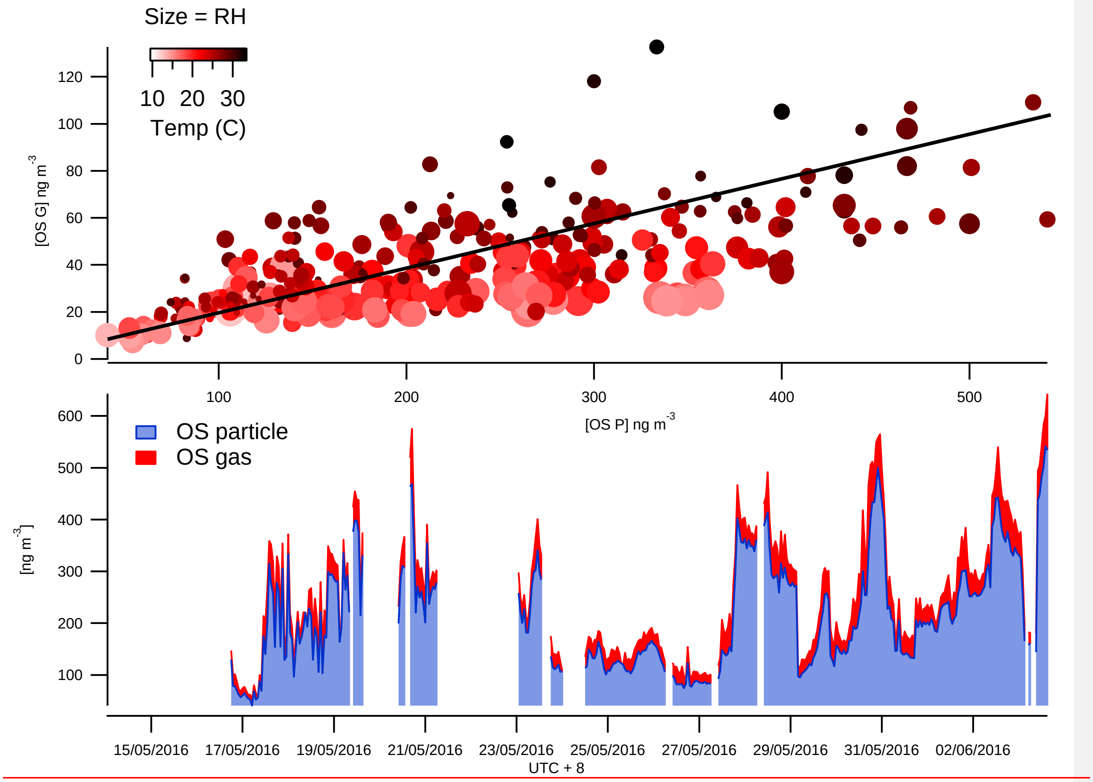

Figure 4. Time series of total SCOs in the gas ~~(SCOG)~~ and particle ~~(SCOP)~~ phase (bottom panel) and their correlation colour coded by temperature and size binned by relative humidity (top panel).

5

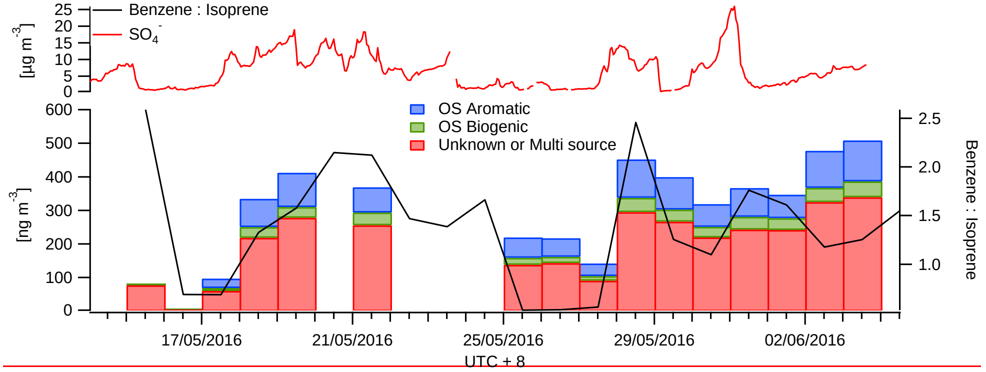

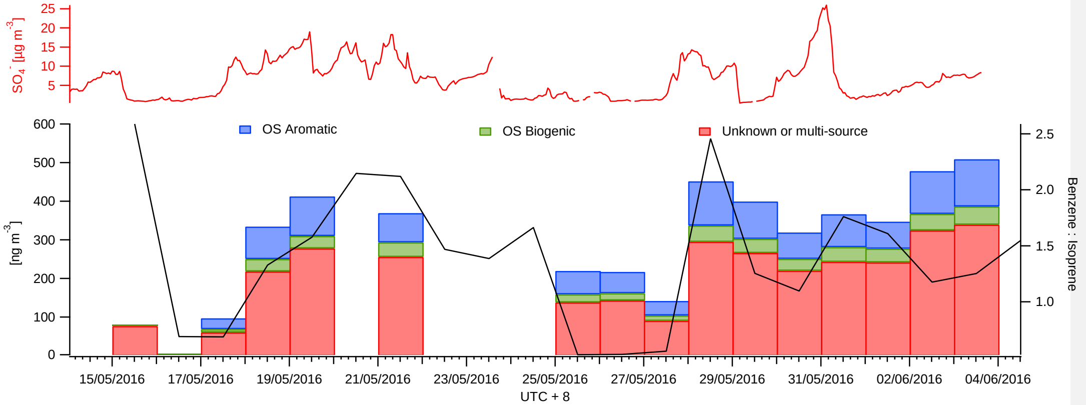

Figure 5. A time series of the mean daily benzene to isoprene ratio as a marker for anthropogenic and biogenic influence (black) is displayed in the top panel. The CIMS data was also binned to provide mean daily SCO concentrations for aromatic (blue) and biogenic (green) precursor SCOs (bottom panel). The red bars represent SCOs with an unknown source or SCO produced via both biogenic and anthropogenic pathways. The AMS SO_4^{2-} concentration is also presented to indicate availability of sulfur in the particle phase.

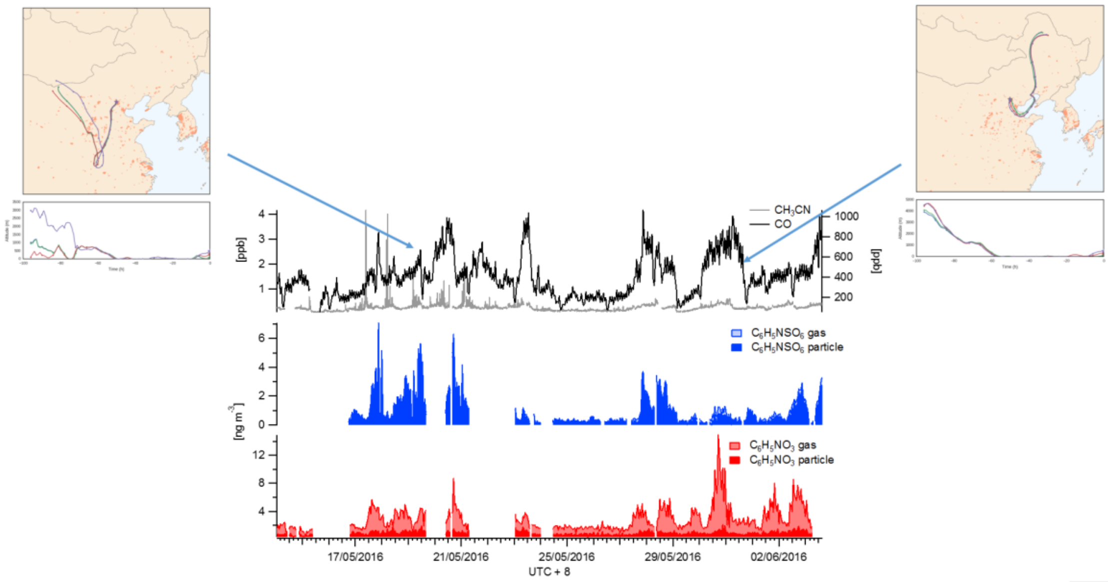
CH$_3$CN
CO
[ppb]
[ppb]
1000
800
600
400
200
C$_6$H$_5$NSO$_6$ gas
C$_6$H$_5$NSO$_6$ particle
[ng m^{-3}]
C$_6$H$_5$NO$_3$ gas
C$_6$H$_5$NO$_3$ particle
17/05/2016
21/05/2016
25/05/2016
29/05/2016
02/06/2016
UTC + 8

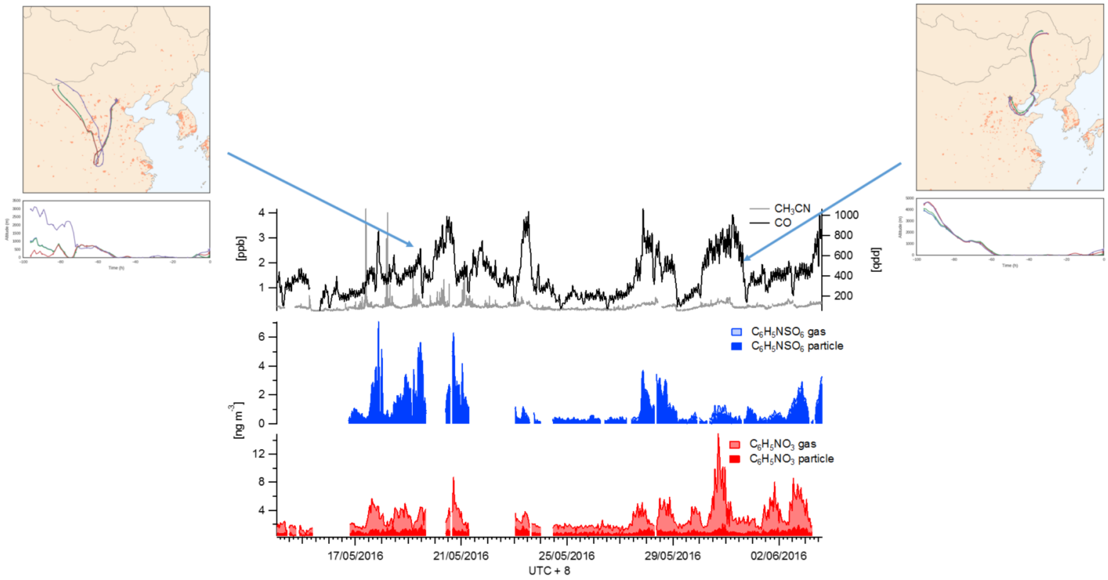
CH$_3$CN
CO
[ppb]
[ppb]
1000
800
600
400
200
C$_6$H$_5$NSO$_6$ gas
C$_6$H$_5$NSO$_6$ particle
[ng m^{-3}]
C$_6$H$_5$NO$_3$ gas
C$_6$H$_5$NO$_3$ particle
17/05/2016
21/05/2016
25/05/2016
29/05/2016
02/06/2016
UTC + 8

Figure 6. Time series of gas and particle phase NP (red), NP OS (blue) and gas phase acetonitrile (grey) and CO (black) between the 16th and 3rd June

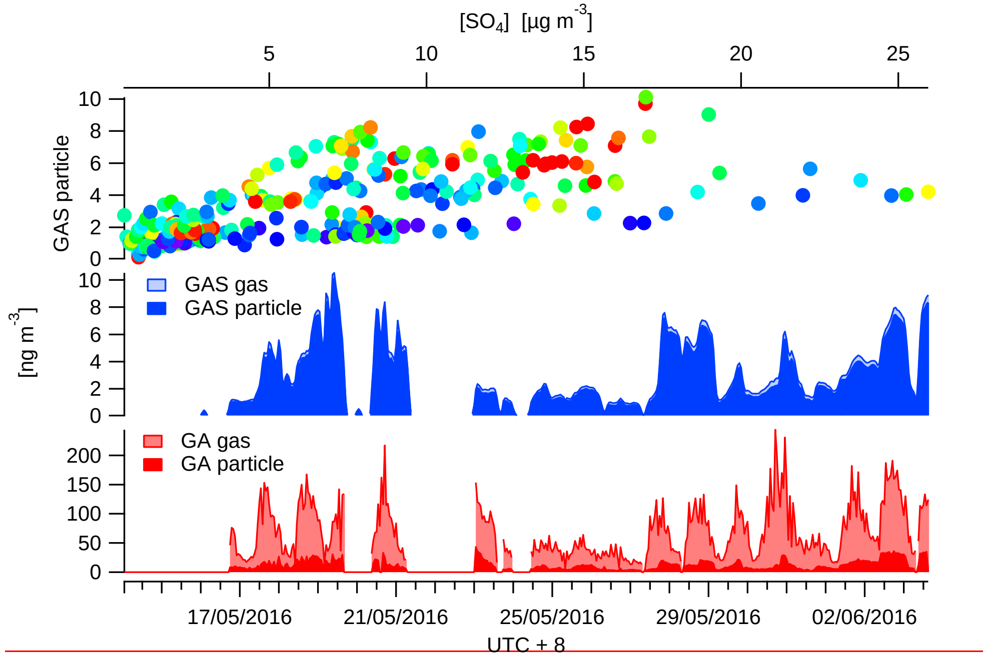

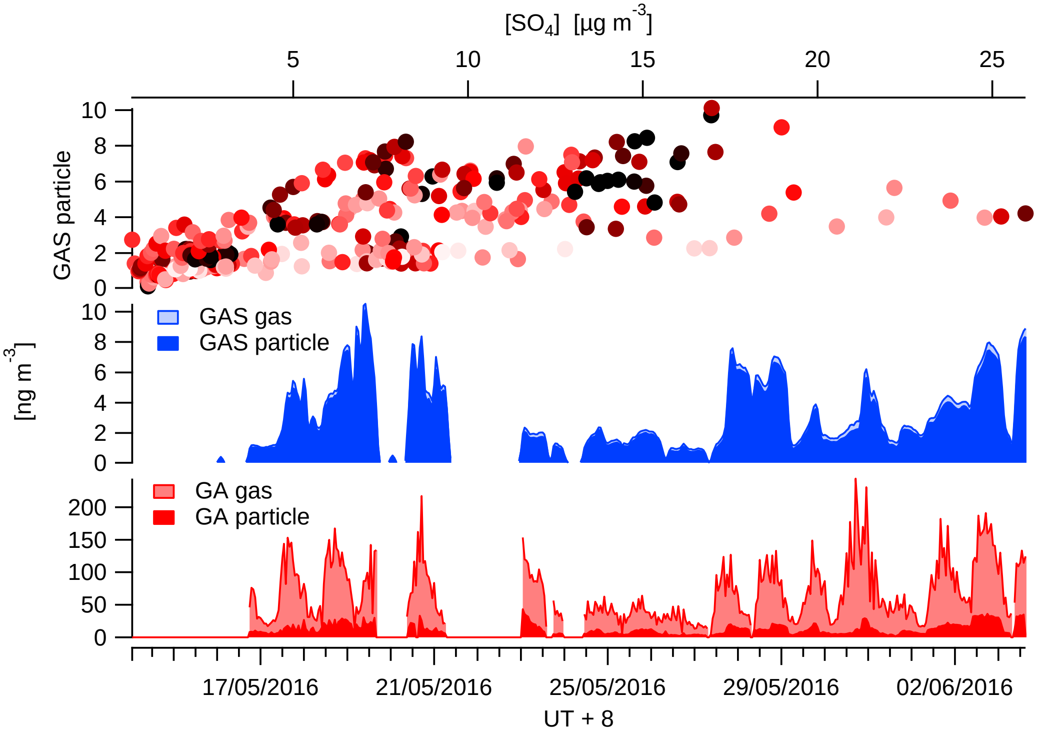

Figure 7. Campaign time series of glycolic acid (red) and GAS (blue) in the particle and gas phase. The top panel illustrates the correlation between GAS in the particle phase and SO_4^{2-} colour coded by GAp/GAg.

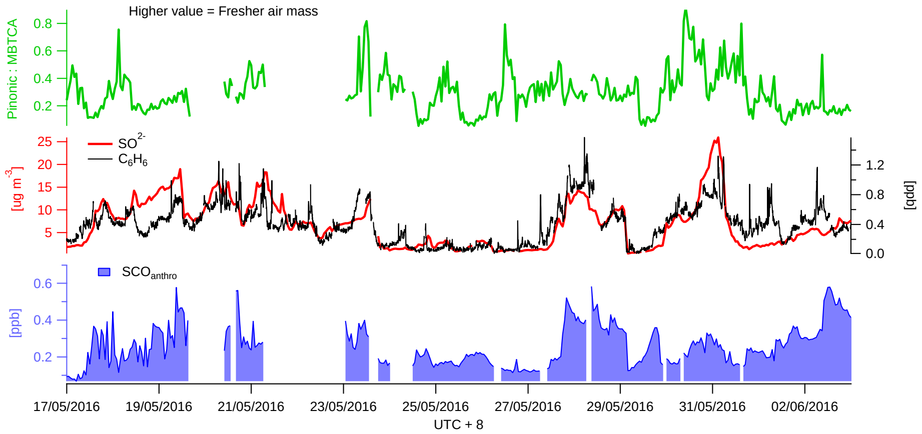

(A)

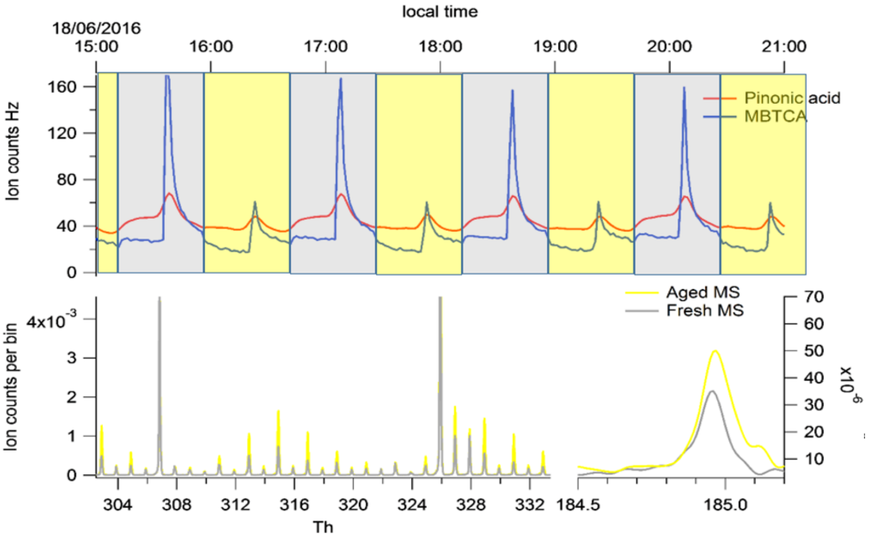

(B)

Figure 8. (A) Total benzene/PAH derived SCO (SCO_{anthro}) time series and respective SO_4^{2-} and benzene concentrations. The indicator of photochemical aging (pinonic acid: MBTCA) is plotted in green. (B) illustrates the mass spectral difference between fresh and aged air masses through Go:PAM and respective time series for pinonic acid and MBTCA.

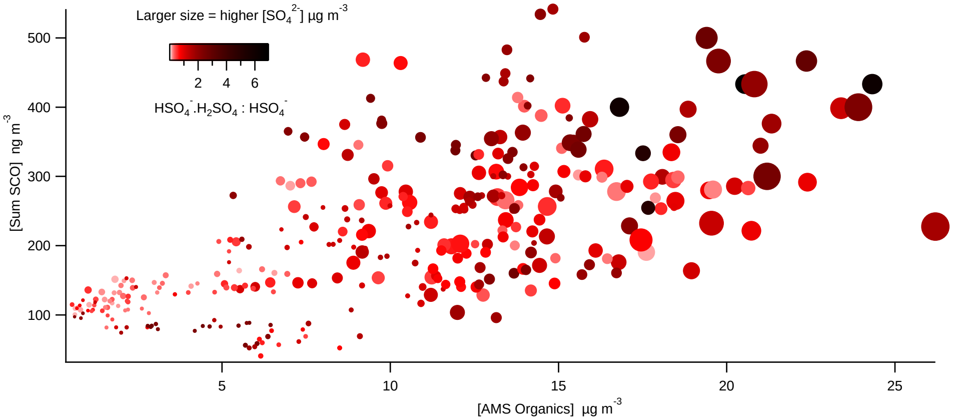

Figure 9. Correlation plot of total SCOs vs total particle phase organics as a function of acidity (colour coding counts of $HSO_4^-.H_2SO_4$: HSO_4) and SO_4^{2-} (data point size spanning concentrations from 0.2 to 16 µg m^{-3}). 5